University of Bristol

University of Bristol - Explore Bristol Research
General rights

PALEOBIOLOGY
A PUBLICATION OF THE
Paleontological
SOCIETY

Geographic and temporal morphological stasis in the latest Cretaceous ammonoid *Discoscaphites iris* from the U.S. Gulf and Atlantic Coastal Plains

James D. Witts* , Corinne E. Myers, Matthew P. Garb, Kayla M. Irizarry, Ekaterina Larina, Anastasia Rashkova, and Neil H. Landman

Abstract.—We examine temporal and spatial variation in morphology of the ammonoid cephalopod *Discoscaphites iris* using a large dataset from multiple localities in the Late Cretaceous (Maastrichtian) of the U.S. Gulf and Atlantic Coastal Plains, spanning a distance of 2000 km along the paleoshoreline. Our results suggest that the fossil record of *D. iris* is consistent with no within-species net accumulation of phyletic evolutionary change across morphological traits or the lifetime of this species. Correlations between some traits and paleoenvironmental conditions as well as changes in the coefficient of variation may support limited population-scale ecophenotypic plasticity; however, where stratigraphic data are available, no directional changes in morphology occur before the Cretaceous/Paleogene (K/Pg) boundary. This is consistent with models of "dynamic" evolutionary stasis. Combined with knowledge of life-history traits and paleoecology of scaphitid ammonoids, specifically a short planktonic phase after hatching followed by transition to a nektobenthic adult stage, these data suggest that scaphitids had significant potential for rapid morphological change in conjunction with limited dispersal capacity. It is therefore likely that evolutionary mode in the Scaphitidae (and potentially across the broader ammonoid clade) follows a model of cladogenesis wherein a dynamic morphological stasis is periodically interrupted by more substantial evolutionary change at speciation events. Finally, the lack of temporal changes in our data suggest that global environmental changes had a limited effect on the morphology of ammonoid faunas during the latest Cretaceous.

James D. Witts. School of Earth Sciences, University of Bristol, Bristol BS8 1RJ, U.K. E-mail: james.witts@bristol. ac.uk

Corinne E. Myers. Department of Earth and Planetary Sciences, University of New Mexico, Albuquerque, New Mexico 87131, U.S.A. E-mail: cemyers@unm.edu

Matthew P. Garb. Earth and Environmental Sciences, Brooklyn College, New York, New York 11210, U.S.A. E-mail: mgarb@brooklyn.cuny.edu

Kayla M. Irizarry. Department of Geosciences, Pennsylvania State University, University Park, Pennsylvania 16802, U.S.A. E-mail: kmi5137@psu.edu

Ekaterina Larina. Department of Earth Sciences, University of Southern California, Los Angeles, California 90018, U.S.A. E-mail: elarina@usc.edu

Anastasia Rashkova and Neil H. Landman. Division of Paleontology (Invertebrates), American Museum of Natural History, New York, New York 10024, U.S.A. E-mail: arashkova@amnh.org, landman@amnh.org

Introduction

Ammonoid cephalopod mollusks (commonly referred to as "ammonites" by Cretaceous ammonoid workers; Wright et al. 1996) are classic organisms for evolutionary studies thanks to their excellent fossil record, high rates of speciation and extinction, and preservation of morphological changes through ontogeny (see references in reviews by De Baets et al. 2015a; Monnet et al. 2015; Yacobucci 2015). It is often argued that they show high levels of morphological/ecophenotypic plasticity similar to modern cephalopods (Doubleday et al. 2016). Intraspecific variability is rarely quantified in ammonoids, particularly
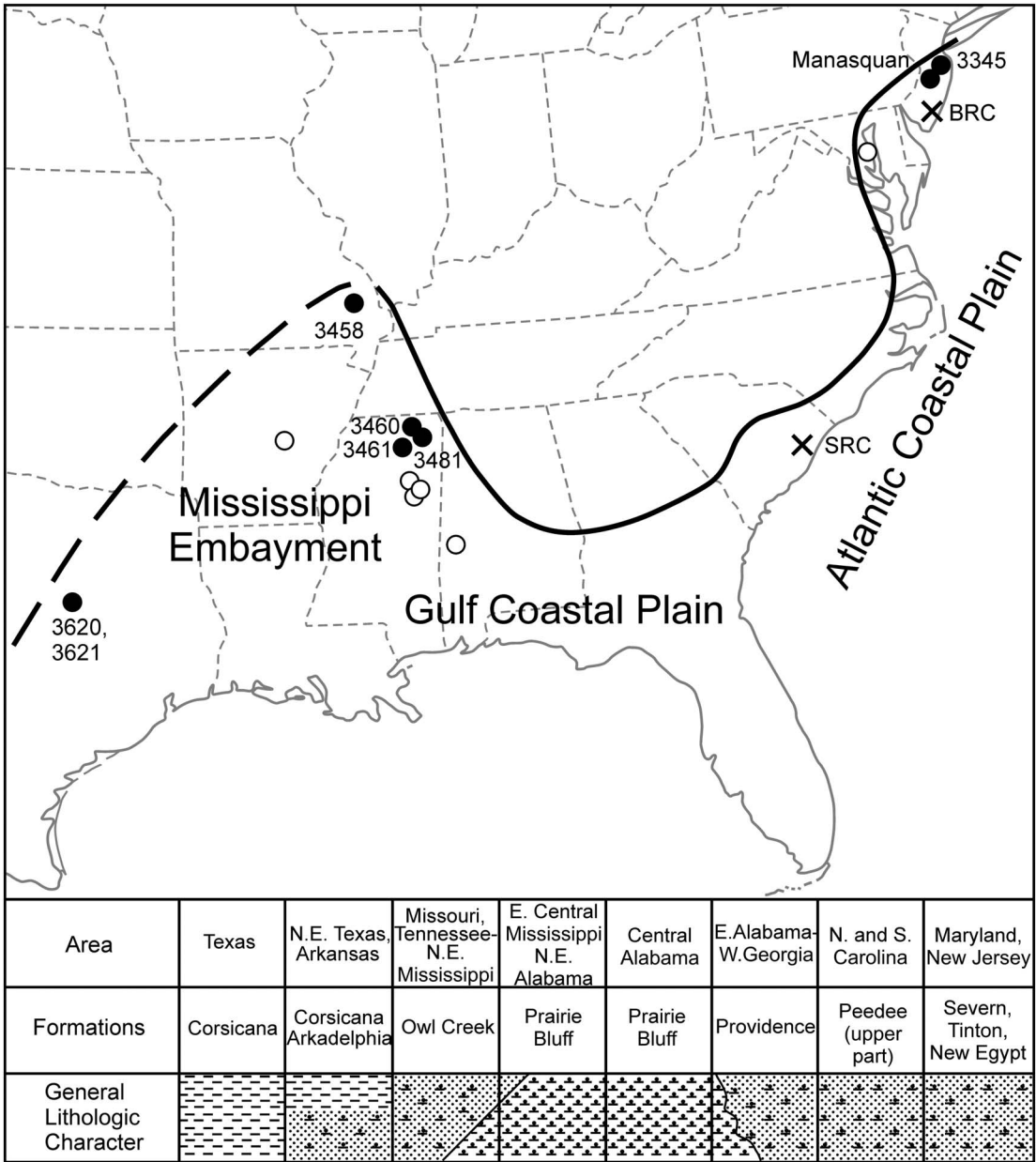
FIGURE 1. Locality map illustrating sites where *Discoscaphites iris* is found across the Atlantic Coastal Plain (ACP) and Gulf Coastal Plain (GCP) (black and white circles). Labeled black circles are sites that yielded specimens for this study. Black crosses are important drill cores used for biostratigraphic correlation of microfossil taxa (see Landman et al. 2004a; Larina et al. 2016). SRC, Santee Reserve Core; BRC, Bass River Core. Lower portion of figure is a cross section (SW–NE) illustrating general lithologic character/facies distribution and formations that contain the *D. iris* Zone across the ACP and GCP.

for "heteromorph" or uncoiled ammonoids (Kakabadze 2004), but their fossil record provides the opportunity to examine large sample sizes geographically and temporally—perfect for testing hypotheses of macroevolutionary change versus stasis in the fossil record.

In this study, we examine the morphology of the ammonoid species *Discoscaphites iris* (family Scaphitidae) across the Atlantic Coastal Plain (ACP) and Gulf Coastal Plain (GCP) of the United States (Fig. 1) using collections from multiple sites. Scaphitid ammonoids are
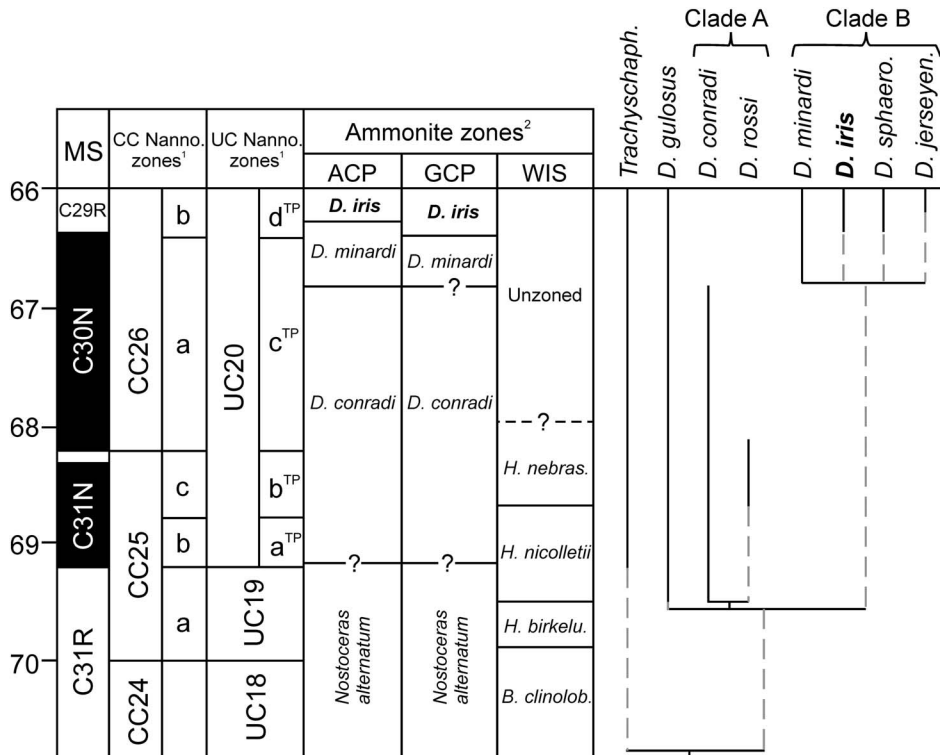
FIGURE 2. Biostratigraphic framework for the Gulf and Atlantic Coastal Plains, USA, based on (1) calcareous nannofossils and (2) ammonite zonation (modified from Larina et al. 2016), with tentative correlation to the Western Interior Seaway (WIS) zonation (based on data in Landman et al. 2004a, 2007; Cobban et al. 2006). Also plotted is the phylogenetic analysis of relationships among North American *Discoscaphites* species from the consensus tree of Landman et al. (2007), with the genus *Trachyscaphites* as the outgroup. Vertical black lines indicate observed stratigraphic ranges. MS, magnetostratigraphy; *B. clinolob.*, *Baculites clinolobatus*; *H. birkelu.*, *Hoploscaphites birkelundae*; *H. nebras.*, *Hoploscaphites nebrascensis*; *Trachyscaph.*, *Trachyscaphites*; *D. sphaero.*, *Discoscaphites sphaeroidalis*; *D. jerseyen.*, *Discoscaphites jerseyensis*.

well preserved, widely distributed, and locally abundant in Late Cretaceous shallow-marine sediments across the Northern Hemisphere (e.g., Landman and Waage 1993; Machalski 2005; Landman et al. 2010, 2014). *Discoscaphites* in particular is one of the last common ammonoid genera found at the end of the Cretaceous (see review by Landman et al. 2015), and in North America, numerous species occur in the Maastrichtian of the ACP, GCP, and the Western Interior Seaway (WIS) (Fig. 2). *Discoscaphites iris* is abundant in upper Maastrichtian sediments across the ACP and GCP and defines the *D. iris* Assemblage Zone—the highest ammonoid biostratigraphic zone in North America (Fig. 2) (Landman et al. 2004a; Larina et al. 2016; Witts et al. 2021). A single fragmentary specimen has also been reported from the upper

Maastrichtian of Libya (Machalski et al. 2009), but this occurrence requires further study, and the species is otherwise unknown outside North America. Our sample from the ACP and GCP therefore represents a well-known and well-delineated "time slice" (see Koch 1996) and provides an opportunity to examine morphological variation in an ammonoid species across virtually its entire geographic and temporal range. These data provide quantitative information on the range, limits, and potential drivers of intraspecific variation and adaptational change (or lack thereof) that characterize an ammonoid species. They also contribute to broader issues of evolutionary tempo during the latest Cretaceous (e.g., the species stasis debate; see Lidgard and Hopkins 2015), and the drivers and predominate mode of ammonoid evolution and speciation

(Wani 2011; Yacobucci 2015). Finally, a better understanding of the intraspecific evolutionary changes of species immediately preceding the end-Cretaceous (K/Pg) mass extinction event will shed light on the abundance and "health" of ammonoid populations immediately before their terminal extinction.

Background.—The *Discoscaphites iris* Zone is characterized in the ACP and GCP by the co-occurrence of the index ammonoid with (1) the calcareous nannofossil *Micula prinsii*—the marker of the uppermost Maastrichtian Sub-zone CC26b in the scheme of Perch-Nielsen (1985) or UC20d^{TP} in the Tethyan scheme of Burnett (1998)—and (2) the dinoflagellates *Palynodinium grallator*, *Disphaerogena carposphaeropsis*, and *Thalassiphora pelagica* (Landman et al. 2004a,b; Larina et al. 2016). It also coincides with planktonic foraminiferal zones CF1 (*Plummerita hantkeninoides*), CF2, and possibly the upper part of CF3 (*Pseudoguembelina hariaensis*) (Abramovich et al. 2011; Witts et al. 2021). These biostratigraphic markers all overlap with the upper part of magnetochron C30N and overlying chron C29R (Landman et al. 2004a; Abramovich et al. 2011; Larina et al. 2016; Witts et al. 2021), the base of which is currently dated at ~340–400 ka before the K/Pg boundary (66.04 Ma) (Fig. 2) (Batenburg et al. 2012; Thibault 2018; Ogg 2020). Although its precise duration is unknown, these combined data constrain the *D. iris* Zone to the last 1 Myr and more likely the last ~400 kyr of the Maastrichtian. As a minimum estimate for its duration, recent cyclostratigraphic analyses in the GCP suggest the *D. iris* Zone could represent as little as 185 kyr (Naujokaitytė et al. 2021).

As previously mentioned, this time interval is of interest due to its proximity to the K/Pg mass extinction event. Although substantial evidence suggests the primary cause of this event is a bolide impact at Chicxulub in the Gulf of Mexico (e.g., Schulte et al. 2010; Hull et al. 2020), the final ~400 kyr of the Maastrichtian are characterized by dynamic environmental changes. These coincide with emplacement of the "main phase" of the Deccan Traps Large Igneous Province (LIP) in India (Schoene et al. 2019; Sprain et al. 2019), linked to a period of rapid global climate warming and cooling (Barnet et al. 2018; Hull et al.

2020; also see Dzombak et al. 2020). Shifts in the distribution, richness, and abundance of various groups of marine plankton occur alongside these climate changes before the K/Pg boundary (Olsson 2001; Thibault 2016; Vellekoop et al. 2019), while morphological changes (dwarfing) and increased fragmentation in some planktonic foraminifera hint at stressful conditions in the oceans (MacLeod et al. 2000; Keller and Abramovich 2009; Henehan et al. 2016; Gilabert et al. 2021). The influence of these environmental changes on ammonoid species has been debated, with some workers suggesting widespread global decline of ammonoids leading into the K/Pg (e.g., Stinnesbeck et al. 2012) and others supporting species' health and even increased abundance during the latest Cretaceous (Landman et al. 2014, 2015; Witts et al. 2015, 2018, 2021).

Methods

To date, *Discoscaphites iris* has been recorded from >15 localities across the ACP and GCP (see summary in Witts et al. 2021). The abundance of specimens at each locality varies due to local differences in preservation and differing sampling intensities. Our final morphometric dataset consists of 328 specimens collected from nine localities in Texas, Missouri, Mississippi, and New Jersey, representing a ~2000 km transect from SW to NE and encompassing the full geographic spread of these occurrences (Fig. 1). Some examples of *D. iris* are illustrated in Supplementary Figures 1 and 2. Specimens are reposited in the collections of the American Museum of Natural History (Division of Paleontology) (AMNH), Department of Earth and Planetary Sciences, University of New Mexico (UNM), U.S. Geological Survey (USGS), Monmouth County Amateur Paleontological Society (MAPS), and the Museum at the Black Hills Institute of Geological Research (MBHI) (full details for each specimen are available in Supplementary Dataset 1). The stratigraphy of most of the localities these specimens are derived from is detailed in the literature (e.g., Landman et al. 2004b, 2007; Larina et al. 2016; Witts et al. 2018, 2021) and briefly reviewed in the following sections; a summary of locality information is provided in Table 1.

TABLE 1. Summary of locality and sample information for sites across the geographic extent of the *Discoscaphites iris* Zone included in this study.

	Brazos River, Falls County, Texas	Crowley's Ridge, Stoddard County, Missouri	Owl Creek type locality, Tippah County, Mississippi	"4th St" quarry, Union County, Mississippi	Ellis Pit, Union County, Mississippi	Monmouth County, New Jersey	Manasquan River basin, New Jersey
AMNH locality no.	3620, 3621	3458	3460	3481	3461	3345	3335, 3372
Lat./long.	31.112468°N, 96.82970°W	37.005278°N, 89.850278°W	34.748611°N, 88.911667°W	34.4975°N, 88.991389°W	34.552452°N, 88.987009°W	40.296222°N, 74.050973°W	40.21211°N, 74.284486°W
Paleolatitude	34.61	38.19	35.81	35.59	35.64	36.89	36.88
Formation	Corsicana	Owl Creek	Owl Creek	Owl Creek	Owl Creek	New Egypt	Tinton
Lithology	Mudstone	Micaceous sandy silt	Micaceous silt and sand	Siltstone and sandstone	Siltstone and sandstone	Glauconitic mudstone	Glauconitic mudstone
% mud/silt	96	47	48	60	54	55	62
% coarse	4	53	52	40	46	45	38
Stratigraphic thickness of *D. iris* Zone studied	2 m	1.5 m	9 m	1.5 m	2 m	?0.2 m	1 m
Total specimens (*N*)	27	57	111	31	19	4	75
Macroconch (*N*)	14	17	58	13	7	2	39
Microconchs (*N*)	13	40	53	18	12	2	36

New Jersey.—The *D. iris* Zone is present at the top of the Tinton and New Egypt Formations, which outcrop in Monmouth County, New Jersey. Both units are glauconite-rich mudstones. At AMNH locality 3345, *D. iris* specimens are derived from the upper 20 cm of the New Egypt Formation below the K/Pg boundary, which at this locality is an unconformable lag deposit (also known as the "Main Fossiliferous Layer") containing reworked macro- and microfossils (Landman et al. 2004b). In the Manasquan River basin (e.g., AMNH localities 3335 and 3372), material comes from the upper 1 m of the Tinton Formation, primarily from the top 20 cm, which is a richly fossiliferous unit known as the "*Pinna* Layer" (Landman et al. 2007). An iridium anomaly occurs at the base of the "*Pinna* Layer," suggesting a conformable K/Pg sequence, but the boundary itself is probably best placed at the top of this unit (see discussion in Landman et al. 2012b). Measurements from AMNH localities 3335, 3345, and 3372 were mostly taken from the published literature (Landman et al. 2004b, 2007) and are combined due to geographic proximity.

Mississippi.—The *D. iris* Zone occurs in both the mixed carbonate-clastic Prairie Bluff Chalk and the laterally equivalent siliciclastic Owl Creek Formation (Fig. 1). A 1.55-m-thick section of the Owl Creek Formation crops out at AMNH locality 3481 in Union County (Witts

et al. 2018), comprising three distinct units: a 52-cm-thick lower, brown-colored muddy sandstone; a 35-cm-thick gray-colored micaceous muddy siltstone; and a 68-cm-thick yellow-colored bioturbated and well-bedded silty sandstone. *Discoscaphites iris* specimens come from both the brown and gray units, which are abundantly fossiliferous. Only fragments were found in the upper, yellow-bedded unit. The K/Pg boundary occurs at the base of the overlying Clayton Formation, which is a 30-cm-thick poorly sorted muddy quartz sand containing rip-up clasts of Owl Creek Formation, bioclasts, and altered Chicxulub impact spherules (Witts et al. 2018). Lithologically similar sediments are also exposed in Union County at AMNH locality 3461, with specimens of *D. iris* abundant in the upper Owl Creek Formation. At this site, the Owl Creek Formation is a ~1-m-thick yellow-colored, bioturbated, and fossiliferous silty sandstone. The K/Pg boundary occurs at the base of the Clayton Formation, which is a 15-cm-thick cross-bedded sandstone that again contains altered Chicxulub impact spherules overlain by a 10-cm-thick bioclastic limestone.

At the Owl Creek type locality in Tippah County (AMNH loc. 3460), *D. iris* occurs throughout a ~9-m-thick succession of bioturbated micaceous siltstones and sandstones with occasional laminated intervals (Larina et al.

2016). Macrofossils at this locality are often found in "pods" that may represent relict burrows and are beautifully preserved with original aragonitic shell material permitting isotopic analyses (e.g., Sessa et al. 2015; Ferguson et al. 2019). The Clayton Formation again overlies the Owl Creek Formation and is composed of 5 m of poorly fossiliferous orange fine-grained quartz sand and intervals of bryozoan-rich bioclastic limestone. The K/Pg boundary is coincident with the unconformable contact at the top of the Owl Creek Formation.

Missouri.—The Owl Creek Formation outcrops along Crowley's Ridge in Stoddard and Scott Counties (Stephenson 1955). The *D. iris* biozone occurs at AMNH locality 3458, which consists of a 1.5-m-thick outcrop of micaceous sandy siltstone overlain by 0.5-m-thick glauconite-rich muddy sandstones of the Danian Clayton Formation. The unconformable contact between these units marks the K/Pg boundary (Dastas et al. 2014). Fossils are abundant in the Owl Creek Formation, and like the Owl Creek type section in Mississippi, often occur in pods that may represent in-filled burrows.

Texas.—Material comes from outcrops along the Brazos River and its tributaries in Falls County that preserve a continuous and expanded record across the K/Pg boundary (Witts et al. 2021). *Discoscaphites iris* were collected from AMNH localities 3620 (Darting Minnow Creek) and 3621 (Cottonmouth Creek), which both contain 1.5- to 2-m-thick outcrops of the upper Corsicana Formation, a fossiliferous dark mudstone. The lower part of the overlying Kincaid Formation contains complex clastic "event deposits" related to the Chicxulub impact event, the base of which marks the K/Pg boundary (Hansen et al. 1987; Hart et al. 2012; Yancey and Liu 2013). Most *D. iris* come from the Corsicana Formation, but one specimen is derived from the basal unit of the K/Pg event deposit.

To assess paleoenvironmental conditions at each locality, grain-size analyses were conducted on bulk sediment samples collected from stratigraphic units or intervals containing *D. iris* specimens (Table 1). Data for localities in New Jersey were taken from the published literature (Landman et al. 2004b, 2007). For other localities, sediment samples were physically disaggregated and mixed with a 6%

hexametaphosphate solution for 10 minutes. They were then wet sieved in a 63 μm sieve to separate sand- and mud-size (<63 μm) fractions, and percentages of these grain-size fractions were then calculated based on weight loss.

Morphometric Measurements.—Morphometric parameters were measured on well-preserved adult specimens and are the same as those described in Witts et al. (2020) for the closely related species *Hoploscaphites nicolletii* (Fig. 3). All measurements were made using electronic calipers (accuracy of 0.01 mm) on actual specimens. The adult shell of *D. iris* consists of two parts, a closely coiled phragmocone and a slightly to strongly uncoiled body chamber. The adult phragmocone is the part of the phragmocone that is exposed in the adult shell. The body chamber consists of the shaft, beginning near the last septum, and a hook terminating at the aperture. The point at which the hook curves backward is called the point of recurvature. Dimorphism is present in *D. iris*, as in all scaphitid ammonoids and many modern cephalopods, and is interpreted as sexual in nature (Landman and Waage 1993; Davis et al. 1996; Landman et al. 2010). The dimorphs are referred to as the macroconch, presumably the
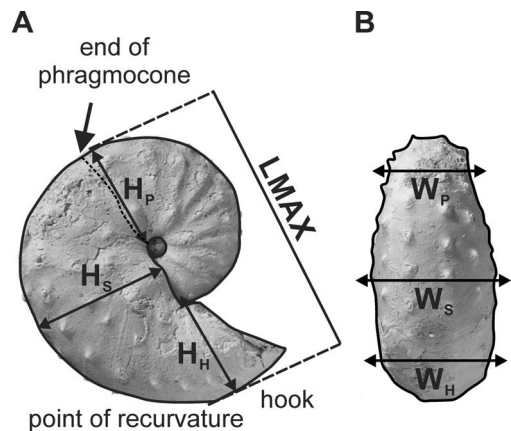
FIGURE 3. Specimen of *Discoscaphites iris* (AMNH 115966—a macroconch—taken from AMNH locality 3460 [Owl Creek type locality, Mississippi]) with explanation of morphometric parameters measured in this study. A, Lateral view showing maximum length (LMAX) and whorl height measurements (H_P, H_S, H_H). B, Ventral view showing whorl width measurements (W_P, W_S, W_H). All measurements are intercostal. See text for further explanation of morphological terminology.

female, and the microconch, presumably the male. Dimorphism is generally expressed by differences in size, robustness, and degree of uncoiling. Results for each dimorph are described separately. A full taxonomic description is available in Supplementary Material.

Maximum length (LMAX) was measured from the venter of the phragmocone to the venter of the hook parallel to the umbilical margin; whorl height was measured at three points on the shell: the end of the phragmocone (H_P), midshaft (H_S), and the point of recurvature (H_H); whorl width was also measured at these same points (W_P, W_S, W_H). The ratios of whorl width to whorl height were calculated at each of these three points (e.g., W_P/H_P) and provide a measure of the degree of whorl compression. Two additional shape ratios were also calculated; the ratio of maximum length to whorl height of the phragmocone along the line of maximum length (LMAX/H_P) is a measure of the degree of uncoiling. The ratio of maximum length to whorl height at midshaft (LMAX/H_S) is a measure of the degree of curvature of the body chamber in lateral view. If the outline of the body chamber in lateral view is a semicircle, the ratio equals 2. The ratio applies only to macroconchs, because the umbilical seam of the body chamber usually coincides with the line of maximum length in these forms, and the whorl height is the distance from the line of maximum length to the venter of the body chamber (equivalent to the radius in the case of a semicircle).

Shape measurements were made at each locality, but whorl compression ratios were not measured on specimens from the Brazos River localities, as these specimens were still embedded in matrix. It is important to note that these data represent variation among mature adults rather than ontogenetic variation (Landman et al. 2008). This is because the mature stage of scaphitid ammonoids is well defined by the uncoiling of the body chamber (e.g., Landman and Waage 1993; Landman et al. 2010); whorl compression ratios taken at different points on the shell provide some information on ontogenetic changes.

Statistical Analyses.—Morphological changes were evaluated using box-and-whisker plots to graphically examine the entire distribution of morphological parameters across the *D. iris* Zone (sensu Monnet et al. 2012). We also calculated the coefficient of variation (CV) for size and shape ratios as well as whorl compression ratios at each site. CV is the standard deviation divided by the mean value of each morphological trait and is often used as a measure of intraspecific variation in ammonoids (e.g., De Baets et al. 2013, 2015a; Klein and Landman 2019). Nonparametric Mann-Whitney *U*-tests were used to evaluate the statistical significance of changes in mean morphological trait values between localities. To correct for multiple comparisons we adjusted *p*-values generated by the Mann-Whitney tests for each morphological trait using three methods. We applied a Bonferroni correction and also controlled for the false discovery rate using the methods of Benjamini and Hochberg (1995) and Benjamini and Yekutieli (2001). Only results considered below are those that were consistently statistically significant across all four of these methods, or at least three out of four methods if the conservative Bonferroni correction did not show significance.

We also explored relationships between morphological traits and several environmental variables available at each locality using linear modeling via the *LM* function in R (R Core Team 2021). Variables considered for each locality were paleolatitude (available using the Paleolatitude Calculator: www.paleolatitude.org; van Hinsbergen et al. 2015) and present-day longitude, which act as reliable proxies for original geographic location and distribution of the samples along the paleoshoreline of the ACP and GCP, and sediment grain size defined as percent of sand-sized material derived from our analyses (Table 1). Grain size varies according to lithology, which itself varies according to numerous factors such as energy level in the environment of deposition, relative water depth, or position relative to shore (Jacobs et al. 1994; Klein and Landman 2019). These physical changes occur along with changes in various biological factors (see "Discussion"). Models were run for each morphological trait and separately for macroconchs and microconchs (Table 2). Separate linear models were also run excluding specimens from the Brazos

TABLE 2. Descriptions of four multiple linear regression models with morphological traits analyzed in each model (size = LMAX; shape = LMAX/H_P, LMAX/H_S; compression = W_P/H_P, W_S/H_S, W_H/H_H), environmental variables, and geographic localities (coded according to U.S. state) analyzed. NJ, New Jersey; MS, Mississippi; MO, Missouri; TX, Texas.

Model	Traits analyzed	Environmental variables	Geographic localities
A (macroconchs)	Size, shape, compression	Paleolatitude, longitude, %sand	NJ, MS, MO, TX
B (microconchs)	Size, shape, compression	Paleolatitude, longitude, %sand	NJ, MS, MO, TX
C (macroconchs)	Size, shape, compression	Paleolatitude, longitude, %sand	NJ, MS, MO
D (microconchs)	Size, shape, compression	Paleolatitude, longitude, %sand	NJ, MS, MO

River localities, which lack shell compression data. All statistical and linear modeling analyses were conducted in R (R Core Team 2021).

Results

The total distribution of size, shape, and shell compression measurements for specimens of *Discoscaphites iris* are illustrated in Figures 4 and 5 as box-and-whisker plots. Plots are arranged geographically from Texas to New Jersey along a general SW-NE transect. For shape traits like maximum length (LMAX) and degree of uncoiling (LMAX/H_P), a clear difference is visible between macroconchs and microconchs at each locality (Fig. 4A,B). Macroconchs are larger than microconchs, while microconchs are more rounded, reflecting the inflated body chamber and straight umbilical margin in macroconchs. All shape traits (also including degree of curvature [LMAX/H_S] for macroconchs; Fig. 4C) show overlap between localities. The ratio of the largest to smallest specimen ranges from 1.14 (AMNH loc. 3461, Ellis Pit) to 1.83 (AMNH loc. 3458, Crowley's Ridge) for macroconchs, and from 1.34 (AMNH loc. 3481, "4th St") to 2.38 (AMNH loc. 3458) for microconchs. Whorl compression ratios also show overlap at all sites between macro- and microconchs (Fig. 5), and between localities across the entire extent of the *D. iris* Zone with no consistent pattern. Full morphological and environmental datasets are available in Supplementary Datasets 2 and 4.

The range of intraspecific variation is similar to estimates from other studies of morphological traits in scaphitids (Landman 1987; Klein and Landman 2019; Witts et al. 2020). Values of the CV for shape traits range from 5% to 21% for both dimorphs and show few clear patterns (Fig. 6, Table 3). Most shape traits show CV values of <10%. LMAX generally

shows the largest variation in both dimorphs (Fig. 6A,B), while LMAX/H_P and LMAX/H_S (for macroconchs) are less variable. Whorl compression CV values in macroconchs range from 7% to 23%, with W_P/H_P (whorl compression at the base of the phragmocone) consistently the most variable (Fig. 6C,D). Microconchs show a similar pattern, with values of CV ranging from 8% to 22%; W_P/H_P again consistently shows the largest variation and W_H/H_H (compression of the hook) the least. Interestingly, CV values for all three whorl compression traits from the Owl Creek type section (AMNH loc. 3460)—the locality with the longest stratigraphic time series—show the smallest range, tightly clustered around 14%. No correlation is observed between CV values and either sample size or stratigraphic thickness of any locality (Supplementary Figs. 3, 4).

The results of pairwise Mann Whitney *U*-tests show that significant differences in morphology of both *D. iris* macro- and microconchs are present between several localities. However, after adjusting *p*-values for multiple comparisons using three different methods (a Bonferroni correction and attempting to control for the false discovery rate using the methodologies of both Benjamini and Hochberg [1995] and Benjamini and Yekutieli [2001]), only five results were consistently statistically significantly different (Table 4). Maximum length (LMAX)—essentially a proxy for size at maturity—of *D. iris* macroconchs between AMNH localities 3460 and (1) AMNH localities 3620/3621 (Brazos River), (2) AMNH locality 3481, and (3) New Jersey localities. In two cases (AMNH loc. 3460 and AMNH loc. 3481 vs. New Jersey localities), macroconchs also show a consistently significant difference in whorl compression at midshaft (W_S/H_S). Five comparisons were statistically significant in three out of four analyses; macroconch LMAX
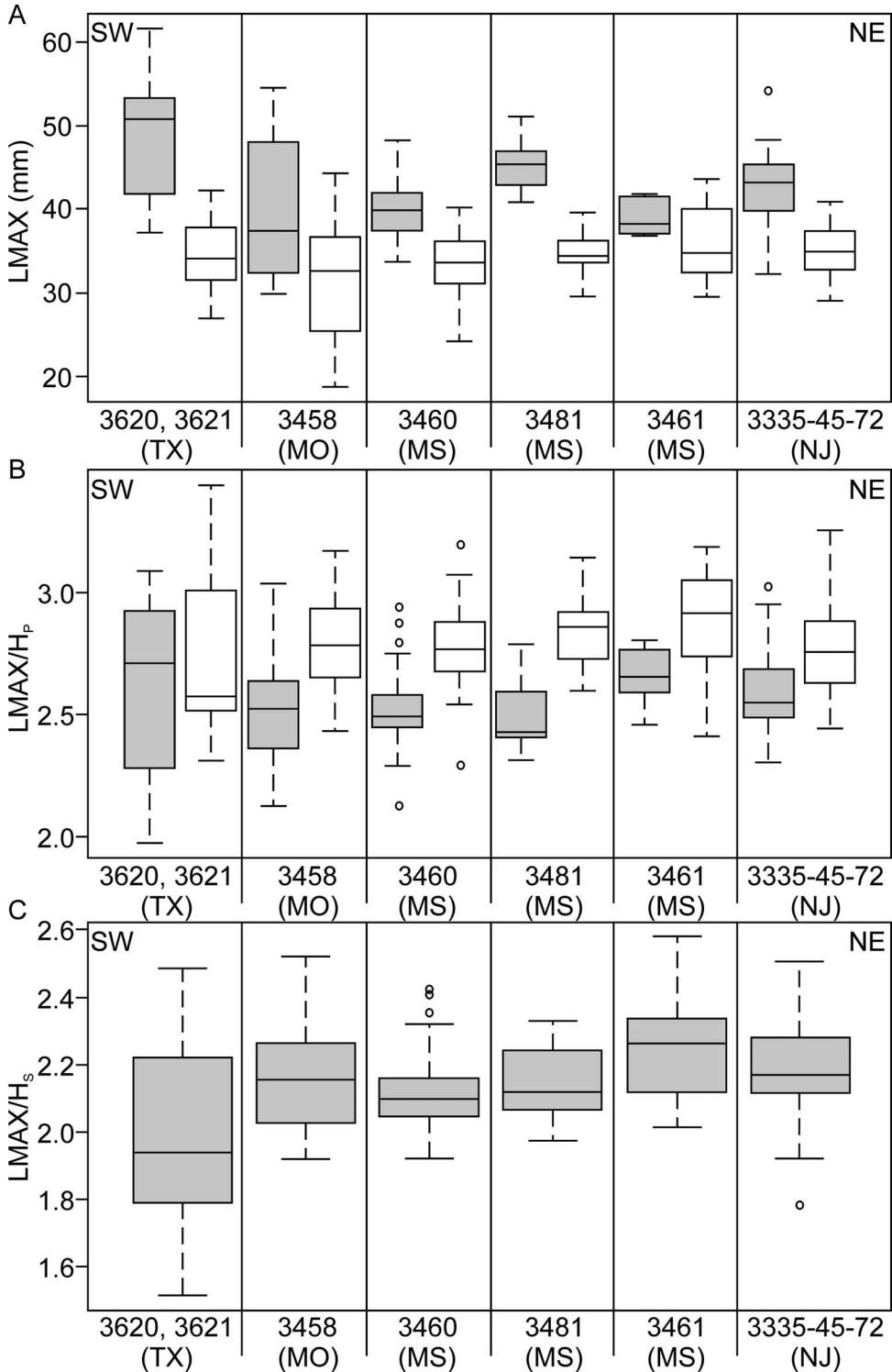
FIGURE 4. Box-and-whisker plots showing size (A, LMAX) and shape ratios (B, LMAX/H_P, C, LMAX/H_S) of *Discoscaphites iris* specimens, plotted geographically from SW (Texas) to NE (New Jersey). Box edges represent the first and third quartile, horizontal black line is the median. Whiskers illustrate the minimum and maximum. Circles are outliers. Data are presented separately for each dimorph; gray shaded boxes are macroconchs, white boxes are microconchs. Note that LMAX/H_S is not measured on microconchs.
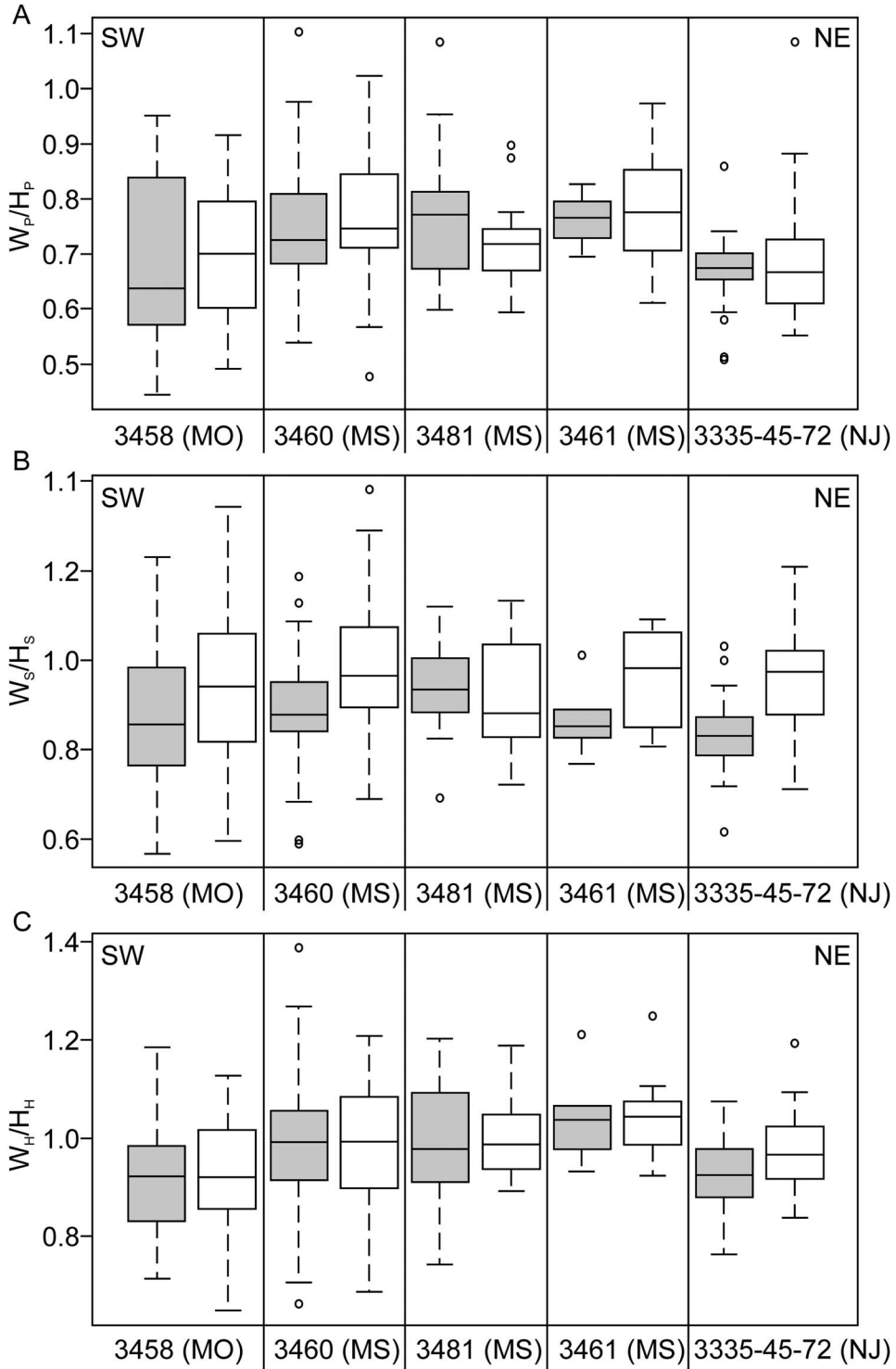
FIGURE 5. Box-and-whisker plots showing whorl compression ratios of *Discoscaphites iris* specimens plotted geographically from SW (Missouri) to NE (New Jersey). A, W_P/H_P, B, W_S/H_S, C, W_H/H_H. Box edges represent the first and third quartile, horizontal black line is the median. Whiskers illustrate the minimum and maximum. Circles are outliers. Data are presented separately for each dimorph; gray shaded boxes are macroconchs, white boxes are microconchs. Compression ratios were not measured on specimens from Brazos River, Texas.

between AMNH locality 3461 and (1) AMNH localities 3481 and (2) 3620/21, (3) macroconch W_P/H_P between AMNH locality 3460 and New Jersey localities, (4) microconch W_P/H_P between AMNH locality 3460 and New Jersey localities, and (5) microconch W_H/H_H between AMNH locality 3461 and AMNH locality 3458. However, comparisons with the conservative Bonferroni correction are statistically significant in none of these cases. All other traits show either no statistically significant differences or a lack of consistency when p-values are corrected for multiple comparisons across the geographic extent of the *D. iris* Zone. Full results of our statistical analyses are available in Supplementary Datasets 3 and 5–7, and all R code is available as part of the Supplementary Material for this paper.

Linear modeling indicates that grain size shows a statistically significant relationship with macroconch LMAX in all models (models A and C) (Table 5). Microconch LMAX also shows a statistically significant relationship with both present-day longitude and paleolatitude when data for all localities are included (model B), but these relationships are not maintained for longitude when data from the Brazos River localities in Texas (AMNH locs. 3620 and 3621) are excluded (model D). Macroconch LMAX shows a significant relationship with paleolatitude, but in this case only when data from Texas are excluded (model C). LMAX/H_P and LMAX/H_S show no significant relationships with environmental variables. Whorl compression at the base of the phragmocone (W_P/H_P) in microconchs shows a statistically significant relationship with paleolatitude and grain size (models B and D). Whorl compression at the hook (W_H/H_H) in both dimorphs shows a significant relationship with paleolatitude (models A–D). Despite these correlations, however, all linear models, including those producing statistically significant relationships, have very low r^2 values (<0.2/20%) (Table 6). The relationship between macroconch LMAX and grain size shows the highest r^2 values, suggesting that it explains 12%–18% variance in models A and C. Overall, these analyses indicate at best a weak relationship with environmental parameters in some traits, with no single

environmental parameter influencing all traits. Model results are illustrated in Supplementary Figures 5–10.

Temporal trends in morphometric data were assessed at AMNH locality 3460 (the Owl Creek type section, Mississippi), which provides the longest continuous stratigraphic record among our localities (Fig. 7) (Sessa et al. 2015; Larina et al. 2016). Data from AMNH localities 3620 and 3621 (Brazos River, Texas) were also plotted against stratigraphy (Fig. 8). Here, data from the Corsicana Formation are presented in a composite section relative to the position of the K/Pg boundary at the base of clastic event deposits in the overlying Kincaid Formation (for details, see Witts et al. 2021). These data generally support the geographic box-and-whisker plots; in both cases, no clear directional trend is apparent in any morphological characters up-section, but a range of variation is present at any given stratigraphic horizon. Likewise, comparison with published paleotemperature estimates at AMNH locality 3460 (Sessa et al. 2015; Ferguson et al. 2019) reveal no trend (Fig. 7D).

Discussion

Ecophenotypy and Intraspecific Variation.— The range of morphometric and CV values at each locality represent varying degrees of intraspecific variation, and together with the occasional significance of paleolatitude and longitude in our linear modeling analysis, suggest that local populations of *Discoscaphites iris* with slightly differing morphologies developed along the shallow margins of the ACP and GCP during the latest Maastrichtian. Despite low statistical support, other trends in our data may support limited local ecophenotypic (plastic) variation in distinct paleoenvironmental settings. For example, the relationship between grain size and maximum length (LMAX) of macroconchs in linear models (Table 5) suggests that size at maturity in this dimorph of *D. iris* varied predictably with this parameter, with smaller specimens more common in more sand-rich environments. There are many factors affecting size at maturity in modern cephalopods that were likely also important in ammonoids (see De Baets et al.
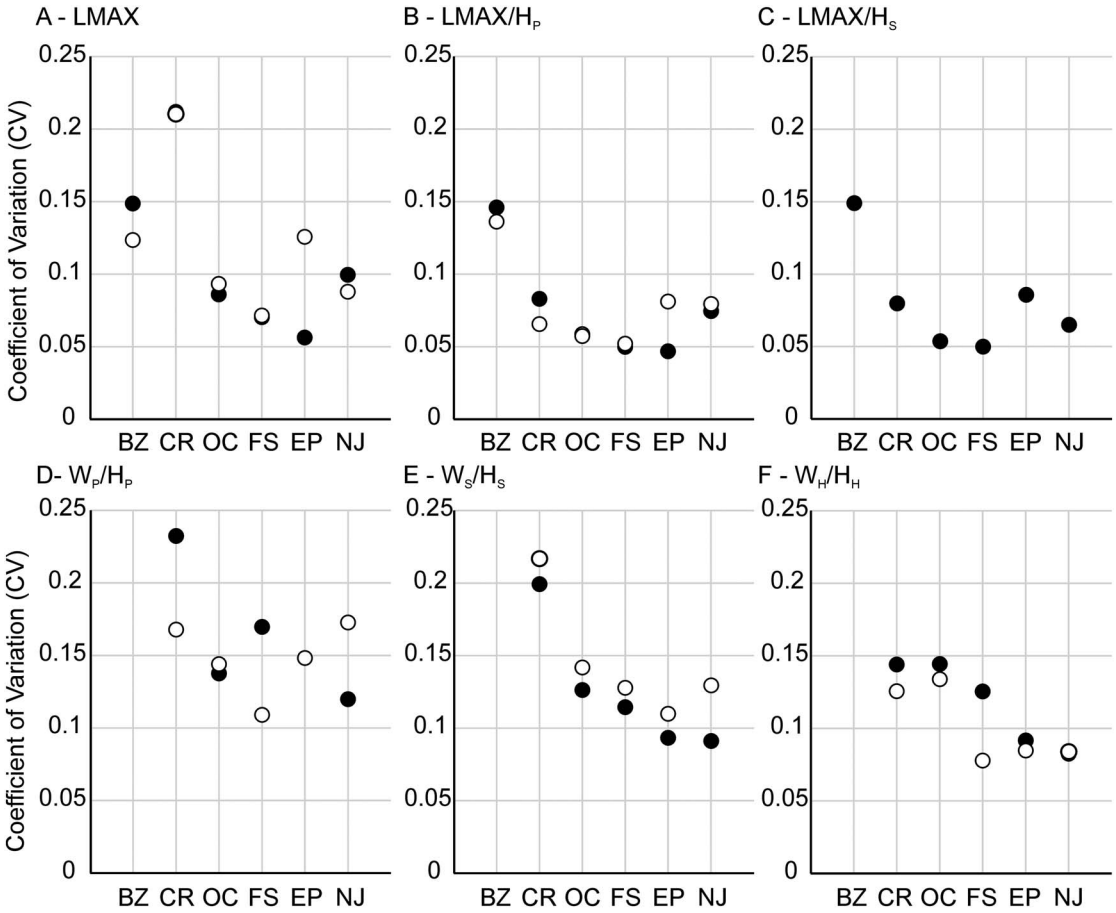
FIGURE 6. Plots showing coefficient of variation (CV) values for shape traits (A–C) and whorl compression traits (D–F). Data are presented separately for macroconchs (black circles) and microconchs (open circles). BZ, Brazos River (AMNH locs. 3620/3621); CR, Crowley's Ridge (AMNH loc. 3458); OC, Owl Creek (AMNH loc. 3460); FS, "4th St" (AMNH loc. 3481); EP, Ellis Pit (AMNH loc. 3461); NJ, New Jersey localities.

TABLE 3. Calculated coefficients of variation (CV) for morphological traits arranged by dimorph and locality. MQ, Manasquan. Gray squares represent no data; LMAX/H_S is only measured in macroconchs. Whorl compression ratios are not available for Brazos River localities.

Locality	Dimorph	LMAX	LMAX/H_P	LMAX/H_S	W_P/H_P	W_S/H_S	W_H/H_H
3335/45/72/MQ (NJ)	Macroconch	0.0995848	0.0745106	0.0649218	0.119865	0.091172	0.082574
	Microconch	0.0878283	0.0794643		0.17283	0.129492	0.083821
3461 (MS)	Macroconch	0.056349	0.046791	0.085621	*0.07059*	0.093383	0.09178
	Microconch	0.125685	0.081107		0.148294	0.109893	0.084726
3481 (MS)	Macroconch	0.0702248	0.0639996	0.0499004	0.169699	0.114439	0.125446
	Microconch	0.0714525	0.0520772		0.109079	0.127826	0.077779
3460 (MS)	Macroconch	0.085965	0.058674	0.0537	0.137724	0.126381	0.144346
	Microconch	0.093204	0.057272		0.144064	0.141882	0.133992
3458 (MO)	Macroconch	0.2118113	0.0828983	0.0797449	0.232404	0.199385	0.143997
	Microconch	0.2103005	0.0654883		0.167929	0.216866	0.125649
3620/21 (TX)	Macroconch	0.1486211	0.145984	0.1489098			
	Microconch	0.1234263	0.136213				

TABLE 4. Morphological traits that show consistent statistically significant differences between localities for macroconchs (M) and microconchs (m). Based on four analyses: Mann-Whitney U-test, analysis of p-values using a Bonferroni correction for multiple comparisons, and assessment of the false discovery rate using the methods of Benjamini and Yekutili (2001) and Benjamini and Hochberg (1995). Italicized results are those that are statistically significant in only 3/4 analyses.

AMNH loc. no.	3335-45-72	3461	3481	3460	3458	3620, 3621
3335-45-72						
3461	-					
3481	W_S/H_S (M)	*LMAX (M)*				
3460	LMAX (M)					
	W_S/H_S (M) W_P/H_P (M + m)	—	LMAX (M)			
3458	—	W_H/H_H (m)	—	—		
3620, 3621	—	*LMAX (M)*	—	LMAX (M)	—	

TABLE 5. Results table highlighting those models (A–D) that resulted in statistically significant relationships between morphological traits and environmental variables at the 95% confidence level. *$LMAX/H_S$ is only measured on macroconchs (models A and C). [†]%silt/mud and %sand were calculated separately but are here combined into a single grain-size variable based on %sand.

	LMAX	$LMAX/H_P$	$LMAX/H_S$*	W_P/H_P	W_S/H_S	W_H/H_H
Paleolatitude	B, C, D			B, D		A, B, C, D
Longitude	B					
Grain-size[†]	A, C			B, D		

TABLE 6. Adjusted r^2 values indicating descriptive power of linear models for each morphological trait examined in this study. *$LMAX/H_S$ is only measured on macroconchs, hence not present in models B and D.

	LMAX	$LMAX/H_P$	$LMAX/H_S$*	W_P/H_P	W_S/H_S	W_H/H_H
Model A	0.1825	0.01082	0.07669	0.07043	0.04773	0.04744
Model B	0.06614	−0.02024	—	0.05705	−0.008156	0.06151
Model C	0.1224	0.01286	0.005594	Same as A	Same as A	Same as A
Model D	0.07025	−0.007068	—	Same as B	Same as B	Same as B

2015a). Grain size is generally considered a proxy for the energy level in the environment of deposition and a rough proxy for relative water depth or position relative to shore (Jacobs et al. 1994; Klein and Landman 2019), which coincides with changes in turbidity, food/nutrient availability, light levels, and even predation and competition. Because LMAX could also signify the age at maturity, it is possible that individuals living in quieter, offshore environments represented by finer-grained sediments grew larger and reached maturity later than those in more nearshore, sandy settings. Flexibility in developmental timing has been hypothesized as a major driver of rapid evolution in ammonoids (Yacobucci 2016), although it is challenging to assess the evolutionary significance of ecophenotypic variations in mollusks (e.g., Grey et al. 2008). LMAX is the trait most likely to show

statistically significant differences between localities in our study (Table 4). This is consistent with the findings of Hopkins and Lidgard (2012), who demonstrated that organismal body size and related traits are particularly labile, with this result consistent across multiple clades.

Previous studies of morphological change in both juvenile and adult scaphitids have noted a consistent pattern of increasing whorl compression in specimens and species from nearshore versus offshore environments—also using grain-size as a proxy (e.g., Jacobs et al. 1994; Klein and Landman 2019; Landman et al. 2020; Witts et al. 2020). Hydrodynamics suggest that a streamlined morphology is more suited to higher-energy conditions in shallow, nearshore settings and that whorl compression is a particularly plastic trait in ammonoids. Statistically significant differences in compression of the body

chamber (W_S/H_S) in *D. iris* macroconchs are present between several localities (Table 4), which are consistent with this hypothesis. The whorl compression trait that shows the largest intraspecific variability in both *D. iris* dimorphs is typically W_P/H_P (Fig. 6). CV values for whorl compression traits from stratigraphically expanded AMNH locality 3460 (Owl Creek type locality) are tightly constrained around 14% in both macro- and microconchs (Fig. 6C,D). This suggests lower levels of ecophenotypic variation in a stable environment, supported by the stratigraphically expanded nature and invariant sedimentology of this section, as well as paleotemperature data (Fig. 7). However, whorl compression values do

not vary with grain size in our linear models, indicating this general relationship between water depth/shell compression is complex and potentially not fully captured using average grain-size data. This calls into question suggestions of a 1:1 relationship between environment and morphology/ecology, which is sometimes assumed in the literature for ammonoid taxa (Westermann 1996; Ritterbush and Bottjer 2012).

It has also been suggested that offshore environments may be more permissible to morphological variations in scaphitids, as populations in these areas did not face the same selective pressures for compressed shells as those in more inshore, higher-energy
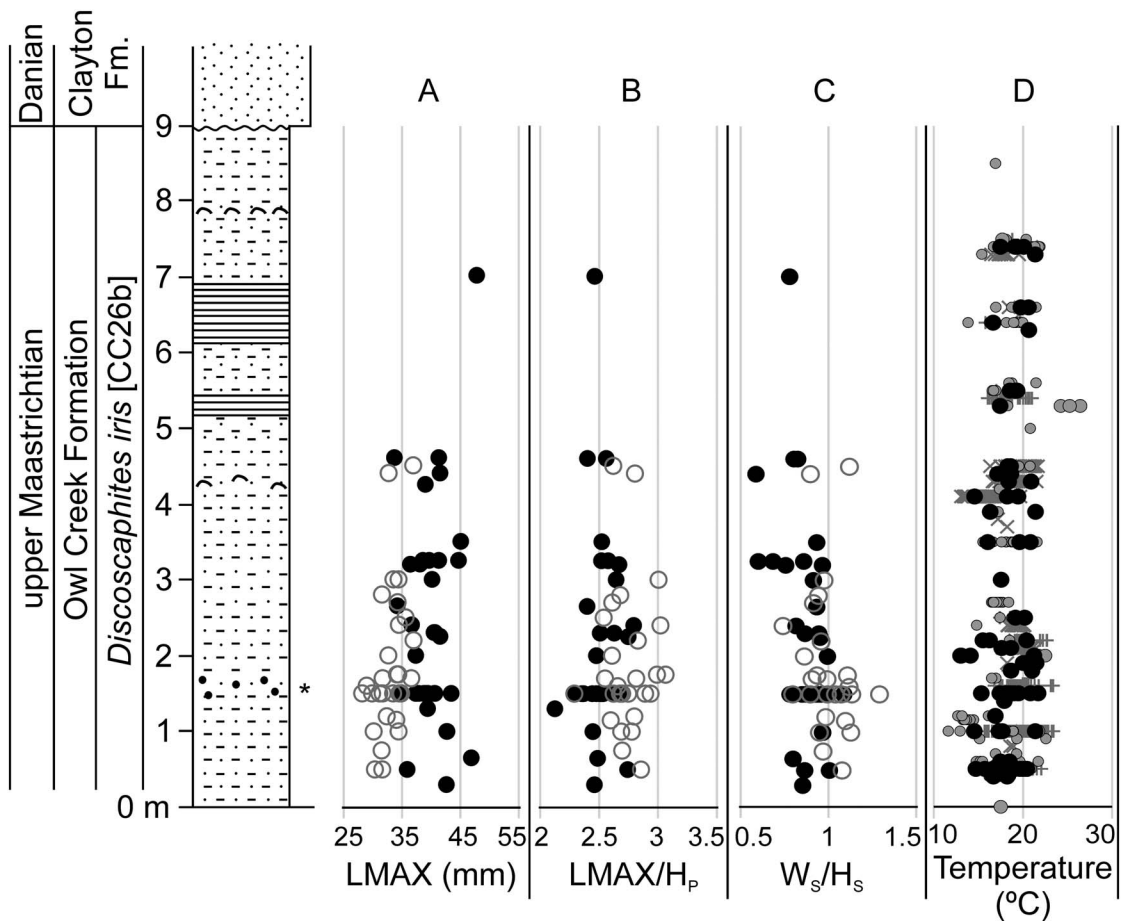

FIGURE 7. Stratigraphic changes in selected *Discoscaphites iris* morphometric traits and paleotemperature at AMNH locality 3460 (Owl Creek type locality, Mississippi). Section modified from Larina et al. (2016). A, LMAX; B, LMAX/H_P; C, W_S/H_S. Filled black circles in A–C are macroconchs, open gray circles are microconchs. D, Paleotemperature data derived from oxygen isotope analysis of various groups of macrofossils (Sessa et al. 2015; Ferguson et al. 2019), converted to temperature using the equation of Grossman and Ku (1986) and assuming a $\delta^{18}O_{seawater}$ value of −1‰). Black circles, scaphitids; gray circles, other ammonoids (baculitids and sphenodiscids); +, infaunal bivalves; ×, epifaunal gastropods and ostreid bivalves.
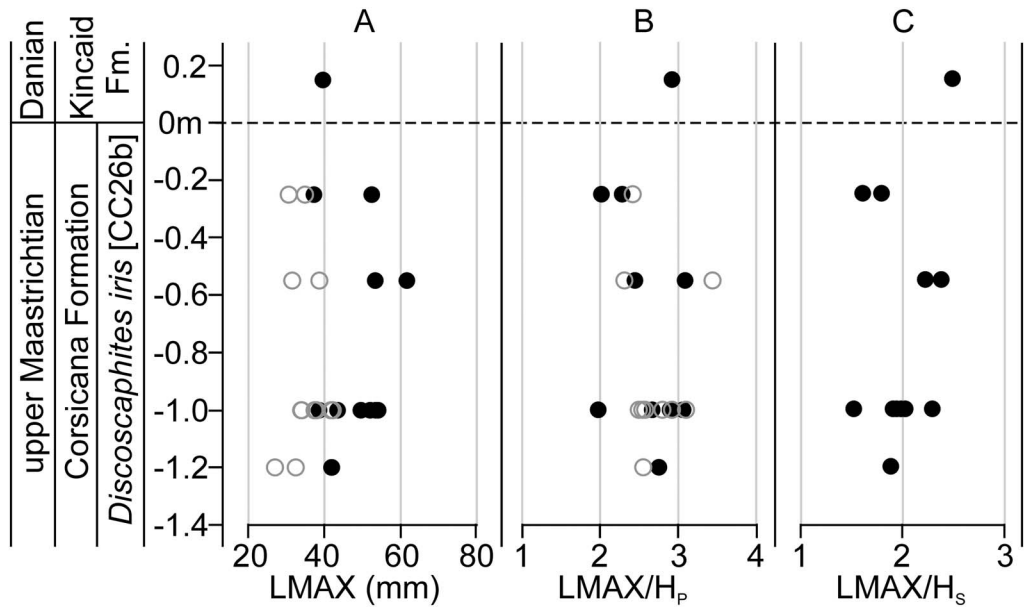
FIGURE 8. Stratigraphic changes in *Discoscaphites iris* morphometric traits below the K/Pg boundary (horizontal dashed line at 0 m) in localities along the Brazos River, Texas. Composite section including data from both AMNH localities 3620 and 3621, with the K/Pg boundary as a datum. See Witts et al. (2021) for more details on the stratigraphy and paleontology of these sites. Filled black circles are macroconchs, open gray circles are microconchs. A, LMAX; B, LMAX/H_P; C, LMAX/H_S (macroconchs only).

environments where such a shape is hydrodynamically favorable (Landman et al. 2020; Peterman et al. 2020). Water-depth estimates for ACP and GCP localities in this study suggest most sites ranged from 20 to 50 m (Landman et al. 2004b, 2007; Sessa et al. 2015; Larina et al. 2016; Witts et al. 2018). It is possible that the higher CV values in size and shape traits for specimens of both dimorphs of *D. iris* from Brazos River are an example of this pattern; estimated water depths for these localities are greater than those for other GCP localities (Hart et al. 2012; Witts et al. 2021). Unfortunately, whorl compression values from this site are not available for comparison.

Effect of Differential Sampling, Time Averaging, and Facies.—It is important to consider the effects of time averaging on these data. Variations in sedimentation/accumulation rates can affect the range of morphological variability within a sample. Hunt (2004) suggested that greatly inflated variance is expected in samples from condensed intervals that accumulated over several tens of thousands of years or that are "lumped" from multiple horizons.

Although all our samples are temporally constrained to within the ~200–500 kyr *D. iris* Zone and can be taken as a single time slice, it is unlikely that all localities are precisely temporally equivalent. *Discoscaphites iris* specimens were collected from restricted stratigraphic intervals (Table 1) <2 m thick, and data are binned at this scale (Figs. 4, 5). The exact duration of these intervals is unknown, and sedimentation rates are clearly variable as reflected in lithological changes (Larina et al. 2016). Landman et al. (2007, 2012b) and Witts et al. (2018) argued that the mode of occurrence of fossils in the "*Pinna* Layer" in New Jersey (AMNH locs. 3335 and 3372) and the "gray unit" at AMNH locality 3481 (which furnished most material in our study from these localities) indicate autochthonous accumulations that formed over short intervals of time and thus provide robust snapshots of in situ marine communities.

Despite temporal uncertainty, CV values for shape traits from the stratigraphically expanded and lithologically homogenous AMNH locality 3460 align closely with those of other,

presumably more condensed, localities and would therefore suggest a similar degree of intraspecific variation despite time averaging (Fig. 4, Fig. 6A,B). Whorl compression traits may differ for other (ecophenotypic) reasons outlined in the previous section. At several localities (e.g., AMNH loc. 3460, AMNH loc. 3458) specimens were commonly found concentrated in fossiliferous pods that may represent hydrodynamic accumulations in seafloor burrow systems (Larina et al. 2016). This, combined with lowered sedimentation rates, could explain the greater range of morphological variability present in samples from AMNH locality 3458.

It should also be noted that our study only contains data from siliciclastic successions across the ACP and GCP. While these sites generally capture the range of environments that *D. iris* occurs in across its geographic range (Fig. 1), the species also occurs in the more carbonate-rich facies of the Prairie Bluff Chalk in Mississippi and Alabama (Larina et al. 2016; Naujokaitytė et al. 2021; Witts et al. 2021). Unfortunately, there are currently too few complete specimens from these localities to usefully compare with siliciclastic successions. This is partly a sampling artifact/bias linked to increased preservation potential for complete specimens in clastic successions, but it may also reflect a true environmental preference whereby *D. iris* is simply more common in siliciclastic environmental settings that tend to represent more nearshore environments. Studies of molluscan occurrence data from the ACP and GCP margins during a comparable latest Maastrichtian time slice (e.g., Sohl and Koch 1983, 1984, 1987) demonstrate lateral changes in the relative abundance of benthic taxa due to shifting paleoenvironments (Fig. 1) (for summaries, see Koch 1996). Further work on the occurrence in different facies and preferred habitat of *D. iris* is needed to test this hypothesis.

"Dynamic Stasis" in Scaphitid Ammonoids: Clues from Modern Cephalopods, Paleoecology, and Phylogeny.—Modern cephalopods are well known for exhibiting morphological plasticity (Boyle and Rodhouse 2005). This is most often related to differing environmental conditions (ecophenotypy) and/or the development of complicated population structures depending on factors such as dispersal or migration ability regulating gene flow (e.g., Boyle and Boletzky 1996; Pérez-Losada et al. 2007; Zaleski et al. 2012; Braga et al. 2017). These features also figure prominently in the debate surrounding plausible mechanisms for speciation and morphological stasis in the fossil record (e.g., Eldredge et al. 2005; Yacobucci 2016). Scaphitids have small embryonic shells suggesting high adult fecundity (Landman 1987; De Baets et al. 2015b), and values of oxygen isotopes in earliest ontogeny are consistent with a surface-water habitat immediately following hatching, presumably as part of the plankton (Linzmeier et al. 2018). During this phase, passive dispersal via ocean currents is plausible, which in the absence of geographic or oceanographic barriers could lead to development of genetic cohesion among well-connected populations. However, this is strongly dependent on the amount of time juvenile ammonoids spent in the plankton (Landman et al. 1996; Villanueva et al. 2016; Wani 2017). There are currently no reliable estimates for growth rates in ammonoids, but rapid growth (reaching maturity in <5 years) is likely (Bucher et al. 1996), which might suggest limited dispersal potential in the plankton. Later-stage juvenile and adult scaphitids were nektobenthic and lived close to the seafloor based on overlap of shell oxygen isotopic data with benthic organisms (Fig. 7) (Sessa et al. 2015; Ferguson et al. 2019); Linzmeier et al. (2018) demonstrated the change from a planktonic to nektobenthic mode of life in scaphitids probably occurred relatively early in ontogeny, at approximately one whorl of postembryonic growth.

Analysis of the functional morphology of shells and well-preserved jaws (aptychi) suggest adult scaphitids exploited a low-energy planktivorous lifestyle (Landman et al. 2010, 2012a). Despite their uncoiled heteromorph shells, scaphitids were capable of active swimming (Peterman et al. 2020), but evidence suggests adults did not undergo long-distance migration. For example, Cochran et al. (2003) found differences in the strontium (Sr) isotopic composition of scaphitid shells from different but laterally equivalent shallow-marine paleoenvironments in the Maastrichtian Fox Hills Formation of the WIS. Yahada and Wani

(2013) examined morphology through ontogeny in samples of scaphitids from laterally equivalent but geographically separate localities in the Turonian of Japan. They found no statistically significant differences in the size of embryonic shells from the two localities but did observe significant differences in the thickness ratio (shell breadth/width) later in ontogeny. They argued that planktonic hatchlings were transported in surface currents between the two localities, but nektobenthic juveniles and adults did not migrate over long distances and formed distinct populations subject to local (ecophenotypic) selective pressures. Taken together, these studies suggest that scaphitids likely had significant potential for rapid morphological change in conjunction with limited dispersal capacity. This combination could fuel rapid evolutionary change (either punctuated, cladogenetic, or phyletic) in scaphitids responding morphologically to unique local environments and limited gene flow between isolated/semi-isolated populations; if paired with speciation, this is an interpretation that fits expectations of the broader ammonoid clade that demonstrates both high diversity and disparity (Yacobucci 2005; Wani 2011).

Our results provide empirical support for morphological stasis in the fossil record of *D. iris* throughout its entire geographic and stratigraphic range, which would suggest a punctuated or cladogenetic mode of evolution in this clade. Preliminary reconstruction of phylogenetic relationships among North American examples of *Discoscaphites* (Landman et al. 2007) and comparison with stratigraphic ranges support this hypothesis (Fig. 2). These data suggest that the geologically older and younger species comprise two clades; *D. iris* belongs to the geologically younger "Clade B" (Fig. 2) and co-occurs with *Discoscaphites minardi*, *Discoscaphites sphaeroidalis*, and *Discoscaphites jerseyensis* in the GCP and ACP. The recently described species *Discoscaphites mullinaxorum* from the upper Maastrichtian of Texas probably also belongs to this clade (Witts et al. 2021). *Discoscaphites minardi* first appears in the GCP and ACP in the middle part of the late Maastrichtian but persists alongside *D. iris* to the K/Pg boundary in the ACP.

"Clade A" contains *Discoscaphites conradi*, *Discoscaphites rossi* (which together form a separate clade), and *Discoscaphites gulosus.* These taxa occur in the ACP, GCP, and WIS in the early late Maastrichtian (Landman and Waage 1993; Landman et al. 2004a; Larina et al. 2016), and *D. gulosus* ranges to the K/Pg boundary (Landman et al. 2007). Morphological stasis in *D. iris*, alongside the co-occurrence of ancestor and/or sister species, lends support for a punctuated or cladogenetic pattern and suggests that anagenesis might not be an important contributor to evolutionary trends in this clade.

It is important to note that potentially ecophenotypic or intraspecific changes outlined above, especially with regard to shifting CV values at each locality, reflect population-scale variability that is not at odds with stasis of the species overall (see discussion in Lieberman et al. 1995; Lieberman 2009). Despite some statistically significant differences between localities, most morphological traits remain invariant across the geographic extent of the *D. iris* Zone and do not exhibit any kind of directional trend in terms of size or shape. Some statistically significant differences in trait values do occur, but there is generally no consistent pattern that might support morphological adaption across time or geography at the species level. In addition, morphological traits show only weak relationships with environmental parameters included in the linear models. Although a limited test of the hypothesis of ecophenotypy, these data do not support strong ecophenotypic variation at the species level. Size, shape, and compression traits measured at the population level also appear to exhibit low levels of intraspecific variation. These results suggest that the fossil record of *D. iris* is consistent with shifting trait values within local populations due to either some limited plastic response to local paleoenvironment or random intrapopulational variation (see discussion De Baets et al. [2015a] for other examples from the ammonoid fossil record), which may simply be compounded by the time-averaging and sampling constraints mentioned earlier.

Despite these caveats, our results clearly support no within-species net accumulation of

phyletic evolutionary change across traits or, where temporal data are available, the lifetime of this species. Notably, data from the Owl Creek type locality (AMNH loc. 3460), the most expanded succession in our dataset, reveal a range of trait values comparable to more restricted sections, with no consistent temporal trends (Fig. 7). Any given stratigraphic horizon at this locality captures a range of variation similar to that of the entire dataset. In addition, paleotemperature estimates based on oxygen isotope analysis of macrofossils (Sessa et al. 2015; Ferguson et al. 2019) show a similar pattern. Both morphology of *D. iris* and the overall paleoenvironment at Owl Creek are consistent with fluctuating regimes around a relatively stable mean but no long-term directional trend. Whereas the precise duration of the Owl Creek stratigraphic section is unknown, the calcareous nannofossil *Micula prinsii* appears at the base of the succession alongside *D. iris* (Larina et al. 2016); as noted earlier, this taxon is restricted to the latest Maastrichtian. In many successions with well-constrained age models, it first occurs within the ~350 kyr interval corresponding to magnetochron C29R (Fig. 2) (Thibault 2018; Gale et al. 2020).

Witts et al. (2020) demonstrated similar statistical support for evolutionary stasis across the temporal and geographic range of another closely related scaphitid ammonoid species, *Hoploscaphites nicolletii*, in the Maastrichtian WIS of North America. More specifically, this study suggested that the fossil record of *H. nicolletii* conforms to the expectations for "dynamic stasis" (e.g., Eldredge et al. 2005; Lieberman 2009); although there were statistically significant morphological changes both temporally and spatially, these were reversible, with a wide range of variation and geographic differences among local populations at any given horizon, some of which could be related to specific environmental conditions (i.e., ecophenotypy) (see also Landman et al. 2008). The exact mechanisms driving patterns of dynamic stasis are still unclear, with both differential selection across paleoenvironments acting in aggregate (Eldredge et al. 2005; Estes and Arnold 2007) or stabilizing selection with a fluctuating optimum associated with shifting environments (Hunt 2007; Hunt and Rabosky 2014) considered plausible by Witts et al. (2020); our results are in good accord with this interpretation. Thus, the study by Witts et al. (2020) also supports a model of punctuated/cladogenetic evolutionary change in scaphitid ammonoids.

Implications of Temporal Stasis for Pre-K/Pg Paleoenvironmental Change.—Size and shape changes documented by other authors in planktonic foraminifera during the latest Maastrichtian, temporally equivalent to the *D. iris* Zone (Larina et al. 2016; Naujokaitytė et al. 2021; Witts et al. 2021), have been related to environmental stresses associated with the emplacement of the Deccan Traps LIP, before the Chicxulub impact event and K/Pg mass extinction (Keller and Abramovich 2009; Henehan et al. 2016; Gilabert et al. 2021). Morphological changes have been detected in ammonoids before other mass extinction events linked to episodes of environmental change driven by LIP volcanism: for example, Kiessling et al. (2018) documented a reduction in size and morphological complexity in ammonoid assemblages from deep-water limestones correlated to the last 700 kyr of the Permian in Iran, coincident with the onset of Siberian Trap LIP volcanism and disruption to the global carbon cycle, but preceding the main phase of the end-Permian mass extinction. However, morphological variation in response to environmental stressors more broadly is a well-studied feature of the ammonoid fossil record. For example, spectacular morphological changes and evolutionary "jumps" within lineages occur during recoveries from carbon cycle perturbations and extinctions (e.g., Monnet et al. 2013), and morphological changes are commonly seen coincident with sea-level fluctuations and faunal invasions in epeiric seaway basins, particularly within endemic lineages (Yacobucci 2003; Klug et al. 2005; Witts et al. 2020).

Although it is difficult to assign a precise age to many samples of *D. iris* below the K/Pg boundary, the stratigraphic data from the Owl Creek type locality outlined earlier suggest no significant directional size or shape changes in this species of ammonoid during the latest Maastrichtian before the K/Pg boundary and

Chicxulub impact event. Limited stratigraphic data from the Brazos River localities (AMNH locs. 3620 and 3621) are also consistent with temporal patterns from Owl Creek in showing no directional trend through time (Fig. 8). Here, *D. iris* co-occurs in the uppermost Corsicana Formation below the K/Pg boundary with the index planktonic foraminifera *Plummerita hantkeninoides*, representing as little as 140 kyr of the latest Maastrichtian (Husson et al. 2014; Gale et al. 2020). In the Manasquan River basin, New Jersey (AMNH locs. 3335 and 3372), *D. iris* and eight other species of ammonite occur in the 20-cm-thick unit known as the "*Pinna* Layer" at the top of the Tinton Formation, associated with a prominent iridium anomaly (Landman et al. 2007). As mentioned earlier, fossils in the "*Pinna* Layer" likely represent a terminal Cretaceous community immediately before the time of the Chicxulub impact (see discussion in Landman et al. 2007, 2012b; Miller et al. 2010). Morphology of *D. iris* from these localities falls within the range of variation seen at other, potentially older, sites (Figs. Fig. 4, 5), again suggesting no differences in size or shape through the duration of the *D. iris* Zone besides the limited population-scale ecophenotypic variations outlined earlier. These results are inconsistent with the LIP-induced ecophenotypic changes proposed for other groups and suggest that any environmental changes related to Deccan volcanism had a limited effect on the morphology of North American ammonoid faunas before the Chicxulub impact and K/Pg mass extinction event.

Conclusions

Research on modern and ancient cephalopods supports the potential for rapid, ecophenotypic morphological change. Moreover, inferred poor larval and adult dispersal ability of scaphitids (Landman et al. 2012a; Yahada and Wani 2013; Linzmeier et al. 2018) increases the likelihood of isolation between populations, which, if combined with morphological change, could promote speciation resulting in high levels of diversity and disparity within the clade. The current paradigm of speciation by some combination of sympatry and micro-allopatry (Wani 2011; Yacobucci 2016), is consistent with this model and the overall pattern of high diversity and disparity in ammonoids more generally. What has remained less clear is how this combination of traits interacts with evolutionary mode to produce the observed patterns (i.e., evolutionary change primarily through phyletic adaptation vs. more punctuated cladogenesis). The results of this analysis indicate that the latest Cretaceous scaphitid *Discoscaphites iris* (like its relative *Hoploscaphites nicolletii*; Witts et al. 2020) demonstrates morphological stasis across its lifetime at the species level and even limited intraspecific variability at the population level. Moreover, no directional changes in species morphology are observed that could be related to contemporaneous Earth system changes during the latest Cretaceous (e.g., environmental stress driven by emplacement of the Deccan Traps LIP) before the K/Pg boundary and Chicxulub bolide impact. It is possible that evolutionary mode in the Scaphitidae follows the punctuated model of cladogenesis, wherein a dynamic morphological stasis is periodically interrupted by more substantial evolutionary change at speciation events. Preliminary phylogenetic analysis of *Discoscaphites* supports this claim. Additional studies that focus specifically on abundance and morphological change across the entire geographic and temporal duration of fossil species (especially those that hypothetically represent ancestors and descendants) could further demonstrate empirically whether the cladogenetic evolutionary mode is indeed pervasive in the highly speciose ammonoid clade or a phenomenon unique to scaphitids. Such work is certainly possible given the nature of the ammonoid fossil record and promises to shed further light on the broader mechanisms of speciation within this diverse clade.

Data Availability Statement

Data available from the Dryad Digital Repository: https://doi.org/10.5061/dryad.jsxksn0br.

Literature Cited

Abramovich, S., G. Keller, Z. Berner, and M. Cymbalista. 2011. Maastrichtian planktic foraminiferal biostratigraphy and paleoenvironment of Brazos River, Falls County, Texas, U.S.A. *In* G. Keller and T. Adatte, eds. The end-Cretaceous mass extinction and the Chicxulub impact in Texas. SEPM (Society for Sedimentary Geology), Tulsa, Okla. SEPM Special Publication 100:123–156.

Barnet, J. S. K., K. Littler, D. Kroon, M. J. Leng, T. Westerhold, U. Röhl, and J. C. Zachos. 2018. A new high-resolution chronology for the late Maastrichtian warming event: establishing robust temporal links with the onset of Deccan volcanism. Geology 46:147–150.

Batenburg, S. M., Sprovieri, A.S. Gale, F.J. Hilgen, S. Hüsing, J. Laskar, D. Liebrand, F. Lirer, X. Orue-Etxebarria, N. Pelosi, and J. Smit. 2012. Cyclostratigraphy and astronomical tuning of the Late Maastrichtian at Zumaia (Basque country, northern Spain). Earth and Planetary Science Letters 359–360:264–278.

Benjamini, Y., and Y. Hochberg. 1995. Controlling the false discovery rate: a practical and powerful approach to multiple testing. Journal of the Royal Statistical Society B 57:289–300.

Benjamini, Y., and D. Yekutieli. 2001. The control of the false discovery rate in multiple testing under dependency. Annals of Statistics 29:1165–1188.

Boyle, P. R., and S. V. Boletzky. 1996. Cephalopod populations: definition and dynamics. Philosophical Transactions of the Royal Society of London B 351:985–1002.

Boyle, P. R., and P. Rodhouse. 2005. Cephalopods: ecology and fisheries. Blackwell Publishing, Oxford.

Braga, R., A. C. Crespi-Abril, S. Van der Molen, M. C. R. S. Bainy, and N. Ortiz. 2017. Analysis of the morphological variation of *Doryteuthis sanpaulensis* (Cephalopoda: Loliginidae) in Argentinian and Brazilian coastal waters using geometric morphometrics techniques. Marine Biodiversity 47:755–762.

Bucher, H., N. H. Landman, S. M. Klofak, and J. Guex. 1996. Mode and rate of growth in ammonoids. Pp. 407–461 *in* N. H. Landman, K. Tanabe, and R. A. Davis, eds. Ammonoid paleobiology. Topics in geobiology, Vol. 13. Springer US, Boston.

Burnett, J. A., with contributions from L. T. Gallagher and M. J. Hampton. 1998. Upper Cretaceous. Pp.132–199 in P. R. Bown, ed. Calcareous nannofossil biostratigraphy. British Micropalaeontological Society Series. Chapman & Hall/Kluwer Academic, London.

Cobban, W. A., I. Walaszczyk, J. D. Obradovich, and K. C. McKinney. 2006. A USGS zonal table for the Upper Cretaceous middle Cenomanian–Maastrichtian of the Western Interior of the United States based on ammonites, inoceramids, and radiometric ages. U.S. Geological Survey Open-File Report 2006-1250.

Cochran, J. K., N. H. Landman, K. K. Turekian, A. Michard, and D. P. Schrag. 2003. Paleoceanography of the Late Cretaceous (Maastrichtian) Western Interior Seaway of North America: evidence from Sr and O isotopes. Palaeogeography, Palaeoclimatology, Palaeoecology 191:45–64.

Dastas, N., J. Chamberlain, and M. Garb. 2014. Cretaceous–Paleogene dinoflagellate biostratigraphy and the age of the Clayton Formation, Southeastern Missouri, USA. Geosciences 4:1–29.

Davis, R. A., N. H. Landman, J.-L. Dommergues, D. Marchand, and H. Bucher. 1996. Mature modifications and dimorphism in ammonoid cephalopods. Pp. 463–539 *in* N. H. Landman, K. Tanabe, and R. A. Davis, eds. Ammonoid paleobiology. Topics in geobiology, Vol. 13. Springer US, Boston.

De Baets, K., C. Klug, and C. Monnet. 2013. Intraspecific variability through ontogeny in early ammonoids. Paleobiology 39:75–94.

De Baets, K., D. Bert, R. Hoffmann, C. Monnet, M. M. Yacobucci, and C. Klug. 2015a. Ammonoid intraspecific variability. Pp. 359–426 *in* C. Klug, D. Korn, K. De Baets, I. Kruta, and R. H. Mapes, eds. Ammonoid paleobiology: from anatomy to ecology. Topics in geobiology, Vol. 43. Springer, Dordrecht, Netherlands.

De Baets, K. D., N. H. Landman, and K. Tanabe. 2015b. Ammonoid embryonic development. Pp. 113–205 *in* C. Klug, D. Korn, K. De Baets, I. Kruta, and R. H. Mapes, eds. Ammonoid paleobiology: from anatomy to ecology. Topics in geobiology, Vol. 43. Springer, Dordrecht, Netherlands.

Doubleday, Z. A., T. A. A. Prowse, A. Arkhipkin, G. J. Pierce, J. Semmens, M. Steer, S. C. Leporati, S. Lourenço, A. Quetglas, W. Sauer, and B. M. Gillanders. 2016. Global proliferation of cephalopods. Current Biology 26:R406–R407.

Dzombak, R. M., N. D. Sheldon, D. M. Mohabey, and B. Samant. 2020. Stable climate in India during Deccan volcanism suggests limited influence on K–Pg extinction. Gondwana Research 85:19–31.

Eldredge, N., J. N. Thompson, P. M. Brakefield, S. Gavrilets, D. Jablonski, J. B. C. Jackson, R. E. Lenski, B. S. Lieberman, M. A. McPeek, and W. Miller. 2005. The dynamics of evolutionary stasis. Paleobiology 31:133–145.

Estes, S., and S. J. Arnold. 2007. Resolving the paradox of stasis: models with stabilizing selection explain evolutionary divergence on all timescales. American Naturalist 169:227–244.

Ferguson, K., K. G. Macleod, N. H. Landman, and J. A. Sessa. 2019. Evaluating growth and ecology in Baculitid and Scaphitid ammonites using stable isotope sclerochronology. Palaios 34:317–329.

Gale, A. S., J. Mutterlose, S. Batenburg, with contributions by F. M. Gradstein, F. P. Agteberg, J. G. Ogg, and M. R. Petrizzio.

2020. The Cretaceous Period. Pp. 1023–1085 *in* F. M. Gradstein, J. G. Ogg, M. D. Schmitz, and G. M. Ogg, eds. Geologic time scale 2020. Elsevier, Amsterdam.

Gilabert, V., I. Arenillas, J. A. Arz, S. J. Batenburg, and S. A. Robinson. 2021. Multiproxy analysis of paleoenvironmental, paleoclimatic and paleoceanographic changes during the early Danian in the Caravaca section (Spain). Palaeogeography, Palaeoclimatology, Palaeoecology 576:110513.

Grey, M., J. W. Haggart, and P. L. Smith. 2008. Species discrimination and evolutionary mode of *Buchia* (Bivalvia: Buchiidae) from Upper Jurassic–Lower Cretaceous strata of Grassy Island, British Columbia, Canada. Palaeontology 51:583–595.

Grossman, E. L., and T. L. Ku. 1986. Oxygen and carbon isotope fractionation in biogenic aragonite: temperature effects. Chemical Geology 59:59–74.

Hansen, T., R. B. Farrand, H. A. Montgomery, H. G. Billman, and G. Blechschmidt. 1987. Sedimentology and extinction patterns across the Cretaceous–Tertiary boundary interval in east Texas. Cretaceous Research 8:229–252.

Hart, M. B., T. E. Yancey, A. D. Leighton, B. Miller, C. Liu, C. W. Smart, and R. J. Twitchett. 2012. The Cretaceous–Paleogene boundary on the Brazos River, Texas: new stratigraphic sections and revised interpretations. GCAGS Journal 1:69–80.

Henehan, M. J., P. M. Hull, D. E. Penman, J. W. B. Rae, and D. N. Schmidt. 2016. Biogeochemical significance of pelagic ecosystem function: an end-Cretaceous case study. Philosophical Transactions of the Royal Society of London B 371:20150510.

Hinsbergen, D. J. J., van, L. V. de Groot, S. J. van Schaik, W. Spakman, P. K. Bijl, A. Sluijs, C. G. Langereis, and H. Brinkhuis. 2015. A paleolatitude calculator for paleoclimate studies. PLoS ONE 10:e0126946.

Hopkins, M. J., and S. Lidgard. 2012. Evolutionary mode routinely varies among morphological traits within fossil species lineages. Proceedings of the National Academy of Sciences USA 109:20520–20525.

Hull, P. M., A. Bornemann, D. E. Penman, M. J. Henehan, R. D. Norris, P. A. Wilson, P. Blum, L. Alegret, S. J. Batenburg, P. R. Bown, T. J. Bralower, C. Cournede, A. Deutsch, B. Donner, O. Friedrich, S. Jehle, H. Kim, D. Kroon, P. C. Lippert, D. Loroch, I. Moebius, K. Moriya, D. J. Peppe, G. E. Ravizza, U. Röhl, J. D. Schueth, J. Sepúlveda, P. F. Sexton, E. C. Sibert, K. K. Śliwińska, R. E. Summons, E. Thomas, T. Westerhold, J. H. Whiteside, T. Yamaguchi, and J. C. Zachos. 2020. On impact and volcanism across the Cretaceous–Paleogene boundary. Science 367:266–272.

Hunt, G. 2004. Phenotypic variation in fossil samples: modelling the consequences of time-averaging. Paleobiology 30:426–443.

Hunt, G. 2007. The relative importance of directional change, random walks, and stasis in the evolution of fossil lineages. Proceedings of the National Academy of Sciences USA 104:18404–18408.

Hunt, G., and D. L. Rabosky. 2014. Phenotypic evolution in fossil species: pattern and process. Annual Review of Earth and Planetary Sciences 42:421–441.

Husson, D., B. Galbrun, S. Gardin, and N. Thibault. 2014. Tempo and duration of short-term environmental perturbations across the Cretaceous–Paleogene boundary. Stratigraphy 11:159–171.

Jacobs, D. K., N. H. Landman, and J. A. Chamberlain, 1994. Ammonite shell shape covaries with facies and hydrodynamics: iterative evolution as a response to changes in basinal environment. Geology 22:905–908.

Kakabadze, M. V. 2004. Intraspecific and intrageneric variabilities and their implication for the systematics of Cretaceous heteromorph ammonids; a review. Scripta Geologica 128:17–37.

Keller, G., and S. Abramovich. 2009. Lilliput effect in late Maastrichtian planktic foraminifera: response to environmental stress. Palaeogeography, Palaeoclimatology, Palaeoecology 284:47–62.

Kiessling, W., M. Schobben, A. Ghaderi, V. Hairapetian, L. Leda, and D. Korn. 2018. Pre–mass extinction decline of latest Permian ammonoids. Geology 46:283–286.

Klein, C., and N. H. Landman. 2019. Intraspecific variation through ontogeny in Late Cretaceous ammonites. American Museum Novitates 2019:1.

Klug, C., W. Schatz, D. Korn, and A. G. Reisdorf. 2005. Morphological fluctuations of ammonoid assemblages from the Muschelkalk (Middle Triassic) of the Germanic Basin—indicators of their ecology, extinctions, and immigrations. Palaeogeography, Palaeoclimatology, Palaeoecology 221:7–34

Koch, C. F. 1996. Latest Cretaceous mollusc species "fabric" of the US Atlantic and Gulf Coastal Plain: a baseline for measuring biotic recovery. Geological Society of London Special Publication 102:309–317.

Landman, N. H. 1987. Ontogeny of Upper Cretaceous (Turonian–Santonian) scaphitid ammonites from the Western Interior of North America: systematics, developmental patterns, and life history. Bulletin of the American Museum of Natural History 195:117–241.

Landman, N. H., and K. M. Waage. 1993. Scaphitid ammonites of the Upper Cretaceous (Maastrichtian) Fox Hills Formation in South Dakota and Wyoming. Bulletin of the American Museum of Natural History 215:1–257.

Landman, N. H., K. Tanabe, and Y. Shigeta. 1996. Ammonoid embryonic development. Pp. 343–4405 *in* N. H. Landman, K. Tanabe, and R. A. Davis, eds. Ammonoid paleobiology. Topics in geobiology, Vol. 13. Springer US, Boston.

Landman, Neil. H., R. O. Johnson, and L. E. Edwards. 2004a. Cephalopods from the Cretaceous/Tertiary boundary interval on the Atlantic Coastal Plain, with a description of the highest ammonite zones in North America. Part 1. Maryland and North Carolina. American Museum Novitates 3454:1–64.

Landman, Neil. H., R. O. Johnson, and L. E. Edwards. 2004b. Cephalopods from the Cretaceous/Tertiary boundary interval on the Atlantic Coastal Plain, with a description of the highest ammonite zones in North America. Part 2. Northeastern Monmouth County, New Jersey. Bulletin of the American Museum of Natural History 287:1–107.

Landman, N. H., R. O. Johnson, M. P. Garb, L. E. Edwards, and F. T. Kyte. 2007. Cephalopods from the Cretaceous/Tertiary boundary interval on the Atlantic Coastal Plain, with a description of the highest ammonite zones in North America. Part 3. Manasquan River Basin, Monmouth County, New Jersey. Bulletin of the American Museum of Natural History 303:1–122.

Landman, N. H., S. M. Klofak, K. B. Sarg. 2008. Variation in adult size of scaphitids ammonites from the Upper Cretaceous Pierre Shale and Fox Hills Formation. Pp. 149–194 *in* P. J. Harries ed. High-resolution approaches in stratigraphic paleontology. Topics in geobiology, Vol. 21. Springer, Dordrecht, Netherlands.

Landman, N. H., W. J. Kennedy, W. A. Cobban, and N. L. Larson. 2010. Scaphites of the "*Nodosus* Group" from the Upper Cretaceous (Campanian) of the Western Interior of North America. Bulletin of the American Museum of Natural History 342:1–242.

Landman, N. H., W. A. Cobban, and N. L. Larson. 2012a. Mode of life and habitat of scaphitid ammonites. Geobios 45:87–98.

Landman, N. H., M. P. Garb, R. Rovelli, D. S. Ebel, and L. E. Edwards. 2012b. Short-term survival of ammonites in New Jersey after the end-Cretaceous bolide impact. Acta Palaeontologica Polonica 57:703–715.

Landman, N. H., S. Goolaerts, J. W. M. Jagt, E. A. Jagt-Yazykova, M. Machalski, and M. M. Yacobucci. 2014. Ammonite extinction and nautilid survival at the end of the Cretaceous. Geology 42:707–710.

Landman, N. H., S. Goolaerts, J. W. M. Jagt, E. A. Jagt-Yazykova, and M. Machalski. 2015. Ammonites on the brink of extinction: diversity, abundance, and ecology of the order Ammonoidea at

the Cretaceous/Paleogene (K/Pg) boundary. Pp. 497–553 *in* C. Klug, D. Korn, K. De Baets, I. Kruta, and R. H. Mapes, eds. Ammonoid paleobiology: from macroevolution to paleogeography. Topics in geobiology, Vol. 44. Springer, Dordrecht, Netherlands.

Landman, N. H., W. J. Kennedy, J. Grier, N. L. Larson, J. W. Grier, T. Linn, L. Tackett, and B. R. Jicha. 2020. Large scaphitid ammonites (Hoploscaphites) from the Upper Cretaceous (Upper Campanian–Lower Maastrichtian) of North America: endless variation on a single theme. Bulletin of the American Museum of Natural History 441:1.

Larina, E., M. Garb, N. Landman, N. Dastas, N. Thibault, L. Edwards, G. Phillips, R. Rovelli, C. Myers, and J. Naujokaityte. 2016. Upper Maastrichtian ammonite biostratigraphy of the Gulf Coastal Plain (Mississippi Embayment, southern USA). Cretaceous Research 60:128–151.

Lidgard, S., and M. J. Hopkins. 2015. Stasis. *In* J. B. Losos, ed. Oxford bibliographies on evolutionary biology. Oxford University Press, New York. http://dx.doi.org/10.1093/OBO/9780199941728-0067.

Lieberman, B. S. 2009. Stephen Jay Gould's evolving, hierarchical thoughts on stasis. Pp. 227–241 *in* W. D. Allmon, P. Kelley, and R. Ross, eds. Stephen Jay Gould: reflections on his view of life. Oxford University Press, New York.

Lieberman, B. S., C. E. Brett, and N. Eldredge. 1995. A study of stasis and change in two species lineages from the Middle Devonian of New York state. Paleobiology 21:15–27.

Linzmeier, B. J., N. H. Landman, S. E. Peters, R. Kozdon, K. Kitajima, and J. W. Valley. 2018. Ion microprobe–measured stable isotope evidence for ammonite habitat and life mode during early ontogeny. Paleobiology 44:684–708.

Machalski, M. 2005. Late Maastrichtian and earliest Danian scaphitid ammonites from central Europe: taxonomy, evolution, and extinction. Acta Palaeontologica Polonica 50:653–696.

Machalski, M., J. W. M. Jagt, N. H. Landman, and J. Uberna. 2009. First record of the North American scaphitids ammonite *Discoscaphites iris* from the upper Maastrichtian of Libya. Neues Jahrbuch für Geologie und Paläontologie 2544:373–378.

MacLeod, N., Ortiz, N., Fefferman, N., Clyde, W., Schulter, C., and J. MacLean. 2000. Phenotypic response of foraminifera to episodes of global environmental change. Pp. 51–78 in S. J. Culver and P. F. Rawson, eds. Biotic response to global environmental change: the last 145 million years. Cambridge University Press, Cambridge.

Miller, K. G., R. M. Sherrell, J. V. Browning, M. P. Field, W. Gallagher, R. K. Olsson, P. J. Sugarman, S. Tuorto, and H. Wahyudi. 2010. Relationship between mass extinction and iridium across the Cretaceous–Paleogene boundary in New Jersey. Geology 38:867–870.

Monnet, C., H. Bucher, J. Guex, and M. Wasmer. 2012. Large-scale evolutionary trends of Acrochordiceratidae Arthaber, 1911 (Ammonoidea, Middle Triassic) and Cope's rule. Palaeontology 55: 87–107.

Monnet, C., H. Bucher, A. Brayard, and J. F. Jenks. 2013. *Globacrochordiceras* gen. nov. (Acrochordiceratidae, late Early Triassic) and its significance for stress-induced evolutionary jumps in ammonoid lineages (cephalopods). Fossil Record 16:197–1215.

Monnet, C., C. Klug, and K. De Baets. 2015. Evolutionary patterns of ammonoids: phenotypic trends, convergence, and parallel evolution. Pp. 95–144 *in* C. Klug, D. Korn, K. De Baets, I. Kruta, and R. H. Mapes, eds. Ammonoid paleobiology: from macroevolution to paleogeography. Topics in geobiology, Vol. 44. Springer, Dordrecht, Netherlands.

Naujokaitytė, J., M. P. Garb, N. Thibault, S. K. Brophy, N. H. Landman, J. D. Witts, J. K. Cochran, E. Larina, G. Phillips, and C. E. Myers. 2021. Milankovitch cyclicity in the latest Cretaceous of the Gulf Coastal Plain, USA. Sedimentary Geology 421:105954.

Ogg, J. G. 2020. Geomagnetic polarity time scale. Pp. 159–192 *in* F. M. Gradstein, J. G. Ogg, M. D. Schmitz, and G. M. Ogg, eds. Geologic time scale 2020. Elsevier, Amsterdam.

Olsson, R. K. 2001. Paleobiogeography of *Pseudotextularia elegans* during the latest Maastrichtian global warming event. Journal of Foraminiferal Research 31:275–282.

Perch-Nielsen, K. 1985. Mesozoic calcareous nannofossils. Pp. 329–426 *in* H. M. Bolli, J. B. Saunders, and K. Perch-Nielsen eds. Plankton stratigraphy. Cambridge University Press, Cambridge.

Pérez-Losada, M., M. J. Nolte, K. A. Crandall, and P. W. Shaw. 2007. Testing hypotheses of population structuring in the Northeast Atlantic Ocean and Mediterranean Sea using the common cuttlefish *Sepia officinalis*. Molecular Ecology 16:2667–2679.

Peterman, D. J., N. Hebdon, C. N. Ciampaglio, M. M. Yacobucci, N. H. Landman, and T. Linn. 2020. Syn vivo hydrostatic and hydrodynamic properties of scaphitid ammonoids from the U.S. Western Interior. Geobios 60:79–98.

R Core Team. 2021. R: a language and environment for statistical computing, Version 4.1.1. R Foundation for Statistical Computing, Vienna, Austria.

Ritterbush, K. A., and D. J. Bottjer. 2012. Westermann morphospace displays ammonoid shell shape and hypothetical paleoecology. Paleobiology 38:424–446.

Schoene, B., M. P. Eddy, K. M. Samperton, C. B. Keller, G. Keller, T. Adatte, and S. F. R. Khadri. 2019. U-Pb constraints on pulsed eruption of the Deccan Traps across the end-Cretaceous mass extinction. Science 363:862–866.

Schulte, P., L. Alegret, I. Arenillas, J. A. Arz, P. J. Barton, P. R. Bown, T. J. Bralower, G. L. Christeson, P. Claeys, C. S. Cockell, G. S. Collins, A. Deutsch, T. J. Goldin, K. Goto, J. M. Grajales-Nishimura, R. A. F. Grieve, S. P. S. Gulick, K. R. Johnson, W. Kiessling, C. Koeberl, D. A. Kring, K. G. MacLeod, T. Matsui, J. Melosh, A. Montanari, J. V. Morgan, C. R. Neal, D. J. Nichols, R. D. Norris, E. Pierazzo, G. Ravizza, M. Rebolledo-Vieyra, W. U. Reimold, E. Robin, T. Salge, R. P. Speijer, A. R. Sweet, J. Urrutia-Fucugauchi, V. Vajda, M. T. Whalen, and P. S. Willumsen. 2010. The Chicxulub asteroid impact and mass extinction at the Cretaceous–Paleogene boundary. Science 327:1214–1218.

Sessa, J. A., E. Larina, K. Knoll, M. Garb, J. K. Cochran, B. T. Huber, K. G. MacLeod, and N. H. Landman. 2015. Ammonite habitat revealed via isotopic composition and comparisons with co-occurring benthic and planktonic organisms. Proceedings of the National Academy of Sciences USA 112:15562–15567.

Sohl, N. F., and C. F. Koch. 1983. Upper Cretaceous (Maestrichtian) Mollusca from the *Haustator bilira* assemblage zone in the East Gulf Coastal Plain. U.S. Geological Survey Open-File Report 83-45:239.

Sohl, N. F., and C. F. Koch. 1984. Upper Cretaceous (Maestrichtian) larger invertebrates from the *Haustator bilira* assemblage zone in the Atlantic Coastal Plain with further data for the East Gulf. U.S. Geological Survey Open-File Report 84-68:282.

Sohl, N. F., and C. F. Koch. 1987. Upper Cretaceous (Maestrichtian) Mollusca from the *Haustator bilira* assemblage zone in the East Gulf Coastal Plain with further data for the east Gulf. U.S. Geological Survey Open-File Report 87-19:172.

Sprain, C. J., P. R. Renne, L. Vanderkluysen, K. Pande, S. Self, and T. Mittal. 2019. The eruptive tempo of Deccan volcanism in relation to the Cretaceous–Paleogene boundary. Science 363:866–870.

Stephenson, L. W. 1955. Owl Creek (Upper Cretaceous) fossils from Crowley's Ridge, southeastern Missouri. U.S. Geological Survey Professional Paper 274:97–140.

Stinnesbeck, W., C. Ifrlm, and C. Salazar. 2012. The Last Cretaceous ammonites in Latin America. Acta Palaeontologica Polonica 57:717–728.

Thibault, N. 2016. Calcareous nannofossil biostratigraphy and turnover dynamics in the late Campanian–Maastrichtian

of the tropical South Atlantic. Revue de Micropaléontologie 59:57–69.

Thibault, N. 2018. Comment on "Extinction, dissolution, and possible ocean acidification prior to the Cretaceous/Paleogene (K/Pg) boundary in the tropical Pacific." Palaeogeography, Palaeoclimatology, Palaeoecology 506:260–262.

Vellekoop, J., L. Woelders, A. Sluijs, K. G. Miller, and R. P. Speijer. 2019. Phytoplankton community disruption caused by latest Cretaceous global warming. Biogeosciences 16:4201–4210.

Villanueva, R., E. A. G. Vidal, F. Á. Fernández-Álvarez, and J. Nabhitabhata. 2016. Early mode of life and hatchling size in cephalopod molluscs: influence on the species distributional ranges. PLoS ONE 11:e0165334.

Wani, R. 2011. Sympatric speciation drove the macroevolution of fossil cephalopods. Geology 39:1079–1082.

Wani, R. 2017. Geological duration of ammonoids controlled their geographical range of fossil distribution. PeerJ 5:e4108.

Westermann, G. E. G. 1996. Ammonoid life and habitat. Pp. 607–707 *in* N. H. Landman, K. Tanabe, and R. A. Davis, eds. Ammonoid paleobiology. Topics in geobiology, Vol. 13. Springer US, Boston.

Witts, J. D., V. C. Bowman, P. B. Wignall, J. Alistair Crame, J. E. Francis, and R. J. Newton. 2015. Evolution and extinction of Maastrichtian (Late Cretaceous) cephalopods from the López de Bertodano Formation, Seymour Island, Antarctica. Palaeogeography, Palaeoclimatology, Palaeoecology 418:193–212.

Witts, J. D., N. H. Landman, M. P. Garb, C. Boas, E. Larina, R. Rovelli, L. E. Edwards, R. M. Sherrell, and J. K. Cochran. 2018. A fossiliferous spherule-rich bed at the Cretaceous–Paleogene (K–Pg) boundary in Mississippi, USA: implications for the K–Pg mass extinction event in the Mississippi Embayment and Eastern Gulf Coastal Plain. Cretaceous Research 91:147–167.

Witts, J. D., N. H. Landman, M. J. Hopkins, and C. E. Myers. 2020. Evolutionary stasis, ecophenotypy and environmental controls on ammonite morphology in the Late Cretaceous (Maastrichtian) Western Interior Seaway, USA. Palaeontology 63:791–806.

Witts, J. D., N. H. Landman, M. P. Garb, K. M. Irizarry, E. Larina, N. Thibault, M. J. Razmjooei, T. E. Yancey, and C. E. Myers. 2021. Cephalopods from the Cretaceous–Paleogene (K-Pg) boundary interval on the Brazos River, Texas, and extinction of the ammonites. American Museum Novitates 3964:1–64.

Wright, C. W., J. H. Calloman, and M. K. Howarth, eds. 1996. Mollusca 4 (revised), Cretaceous Ammonoidea, Vol. 4. Part L of R. C. Moore, ed. Treatise on invertebrate paleontology. Geological Society of America, Boulder, Colo., and University of Kansas Press, Lawrence.

Yacobucci, M. M. 2003. *Neogastroplites* meets *Metengonoceras*: morphological response of an endemic hoplitid ammonite to a newer invader in the mid-Cretaceous Mowry Sea of North America. Cretaceous Research 25:927–944.

Yacobucci, M. M. 2005. Multifractal and white noise evolutionary dynamics in Jurassic–Cretaceous Ammonoidea. Geology 33:97.

Yacobucci, M. M. 2015. Macroevolution and Paleobiogeography of Jurassic–Cretaceous Ammonoids. Pp. 189–228 *in* C. Klug, D. Korn, K. De Baets, I. Kruta, and R. H. Mapes, eds. Ammonoid paleobiology: from macroevolution to paleogeography. Topics in geobiology, Vol. 44. Springer, Dordrecht, Netherlands.

Yacobucci, M. M. 2016. Towards a model for speciation in ammonoids. Pp. 238–277 *in* W. D. Allmon and M. M. Yacobucci eds. Species and speciation in the fossil record. University of Chicago Press, Chicago.

Yahada, H., and R. Wani. 2013. Limited migration of scaphitid ammonoids: evidence from the analyses of shell whorls. Journal of Paleontology 87:406–412.

Yancey, T. E., and C. Liu. 2013. Impact-induced sediment deposition on an offshore, mud-substrate continental shelf, Cretaceous–Paleogene boundary, Brazos River, Texas, U.S.A. Journal of Sedimentary Research 83:354–367.

Zaleski, T., J. A. A. Perez, and A. Luiza Gandara-Martins. 2012. Morphological and morphometric variability of the squid *Lolliguncula brevis* (Mollusca: Cephalopoda) in Brazilian waters: evidence for two species in the western Atlantic? Anais da Academia Brasileira de Ciências 84:1015–1028.